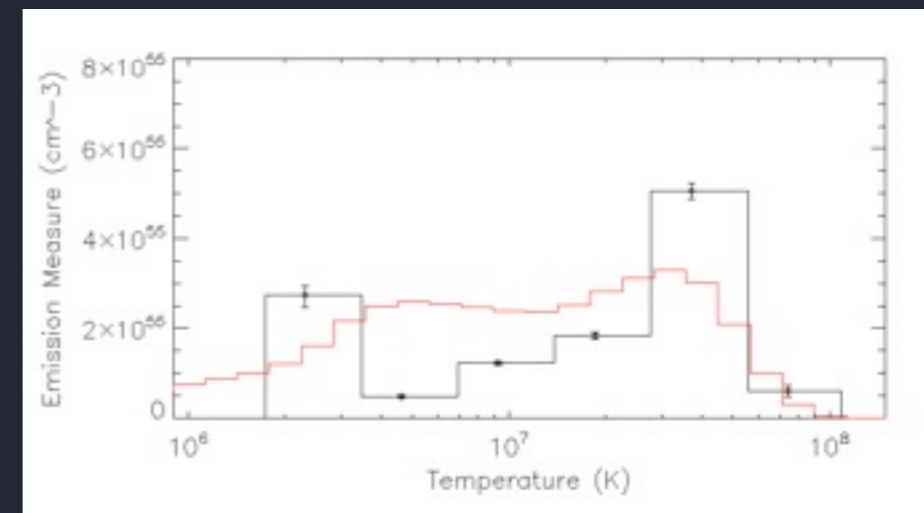
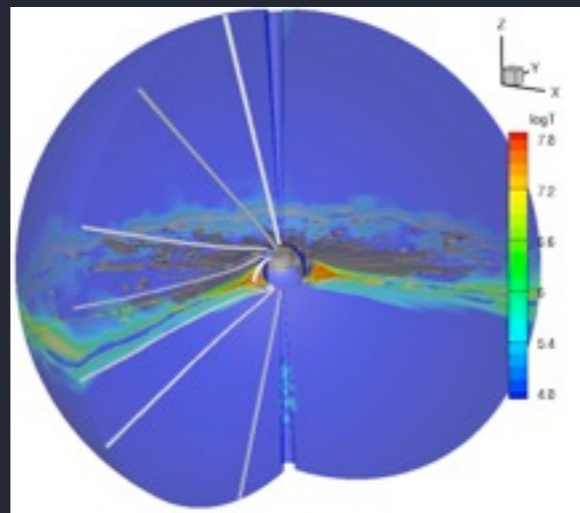
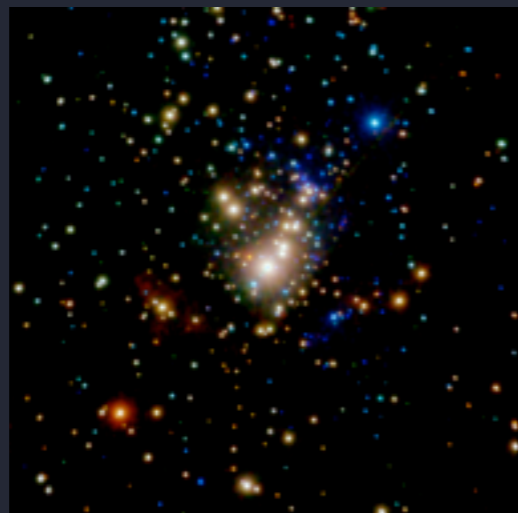
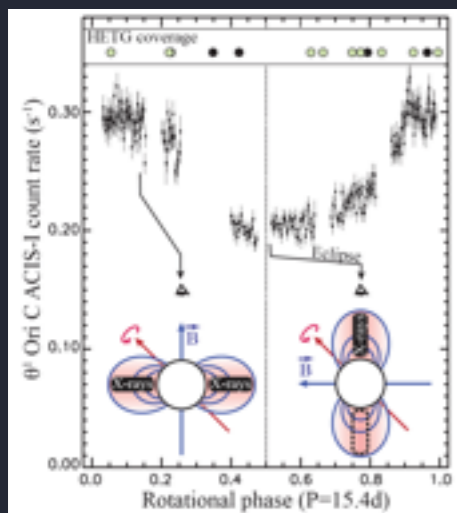


Update on θ^1 Ori C: the Magnetically Confined Wind Shock model does a pretty good job

David Cohen
Department of Physics & Astronomy
Swarthmore College

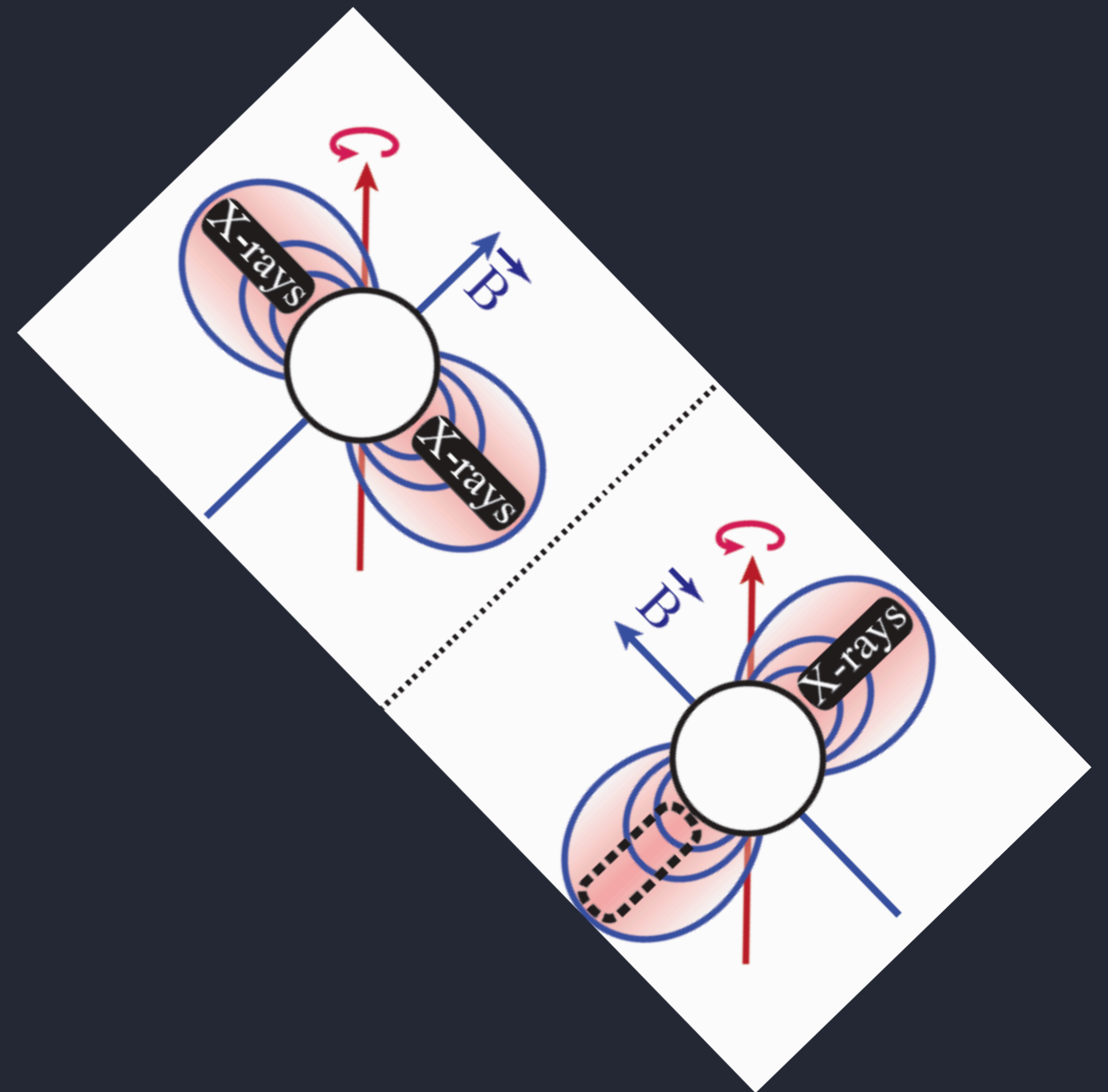
Asif ud-Doula, Véronique Petit, Stan Owocki,
Maurice Leutenegger, Marc Gagné, and
Jackie Pezzato (Swarthmore '17), Randy Doyle (Swarthmore '16)



Outline/overview:

θ^1 Ori C is a magnetic prototype: tilted dipole, slow rotator, moderate confinement ($\eta_* \sim 20$)

X-rays trace the dissipation of wind KE in the magnetosphere



Properties of θ^1 Ori C

O7V (but with some reported variation)

age < 1 Myr

$T_{\text{eff}} \sim 42,000$ K

luminosity $\sim 10^{5.4} L_{\text{sun}}$

$\dot{M} \sim 5 \times 10^{-7} M_{\text{sun}}/\text{yr}$

$v_{\infty} \sim 2500$ km/s

tilted dipole, $B_p \sim 1$ kG

$i \sim \beta \sim 45^\circ$



Properties of θ^1 Ori C

O7V (but with some reported variation)

age < 1 Myr

$T_{\text{eff}} \sim 42,000$ K

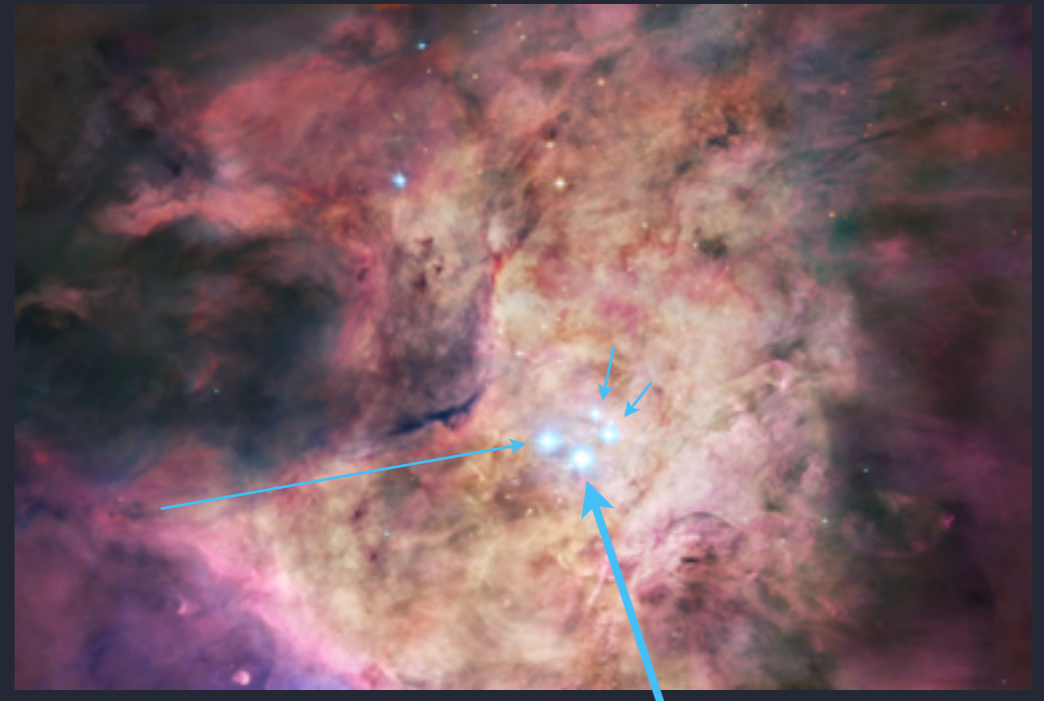
luminosity $\sim 10^{5.4} L_{\text{sun}}$

$\dot{M} \sim 5 \times 10^{-7} M_{\text{sun}}/\text{yr}$

$v_{\infty} \sim 2500$ km/s

tilted dipole, $B_p \sim 1$ kG

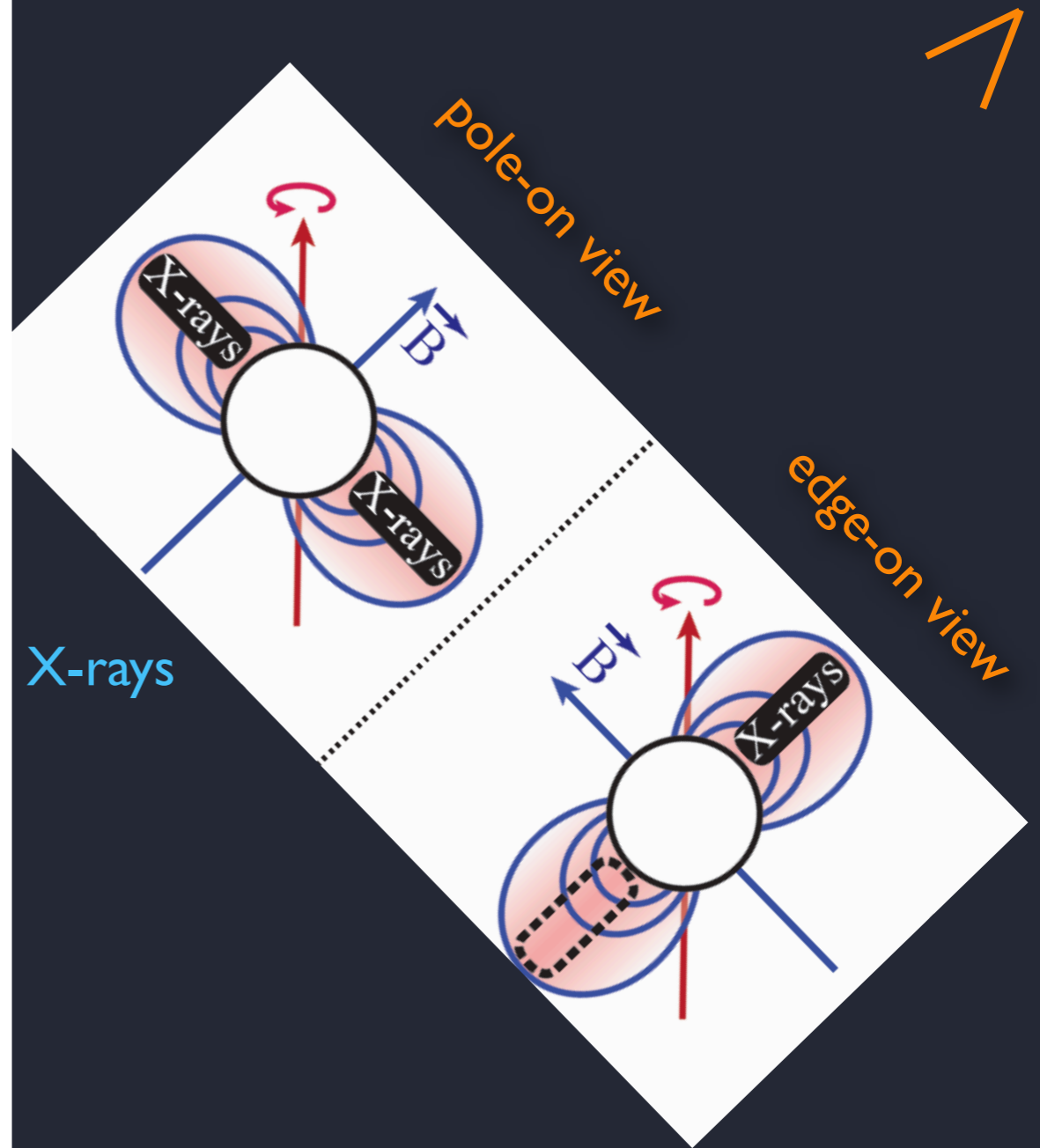
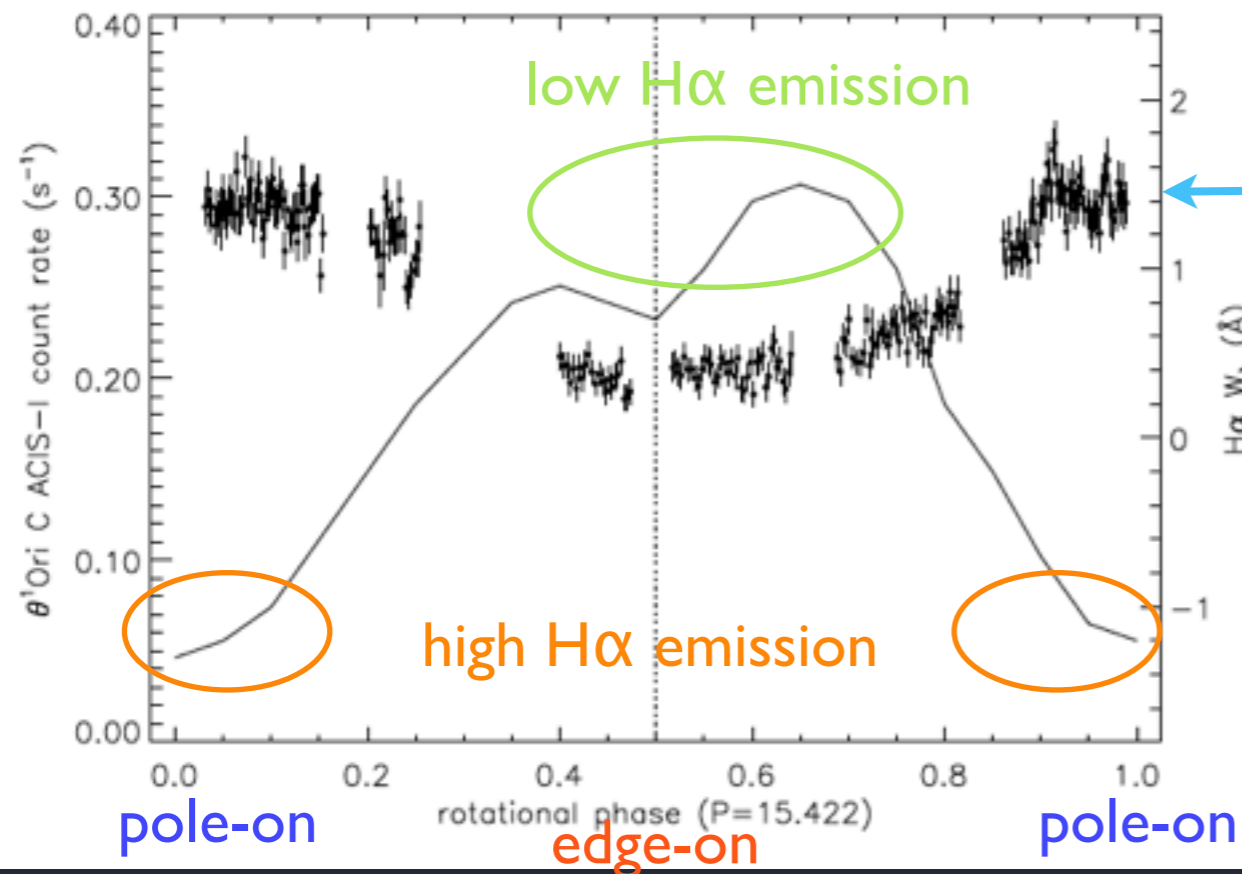
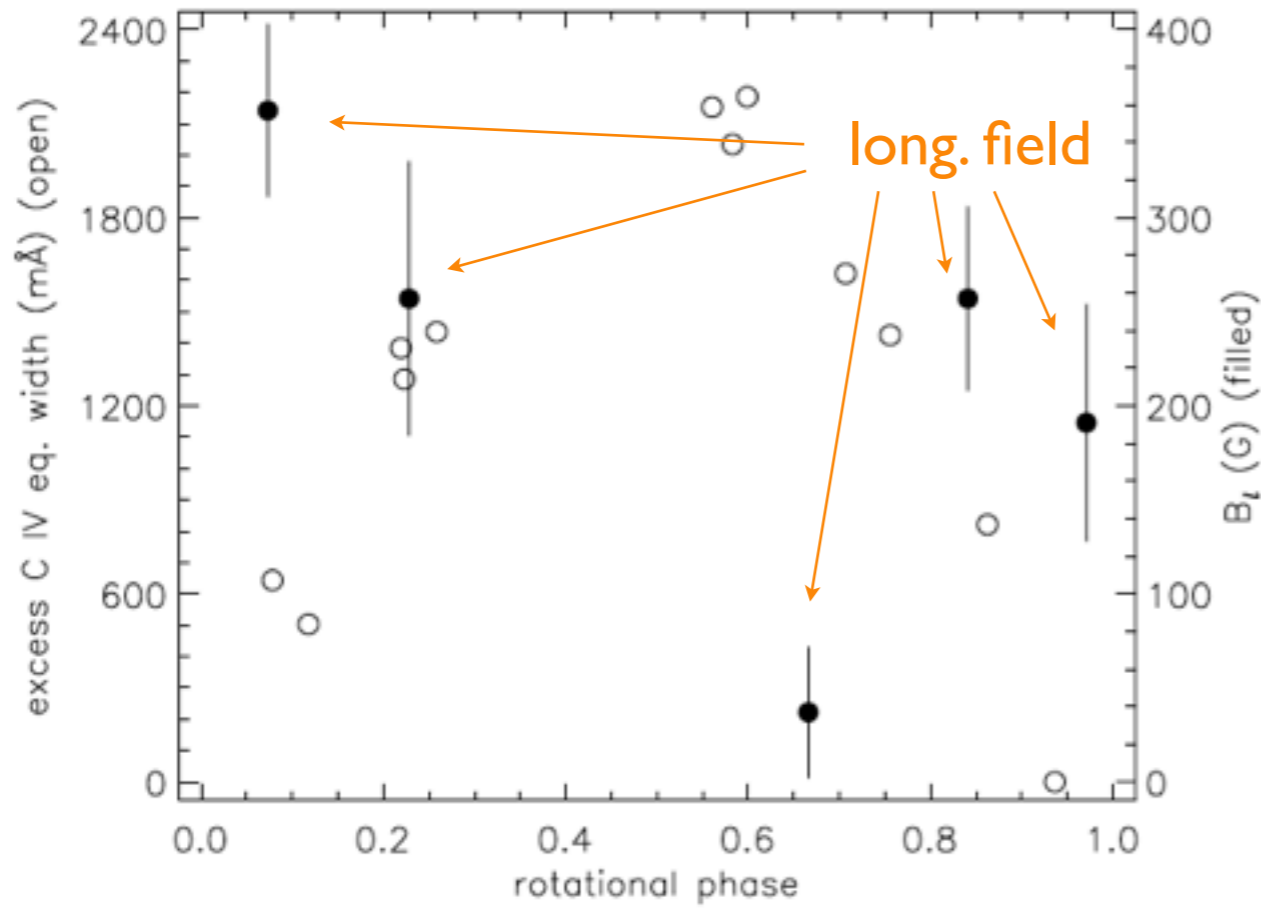
$i \sim \beta \sim 45^\circ$



θ^1 Ori C

One of only two O stars in the ONC

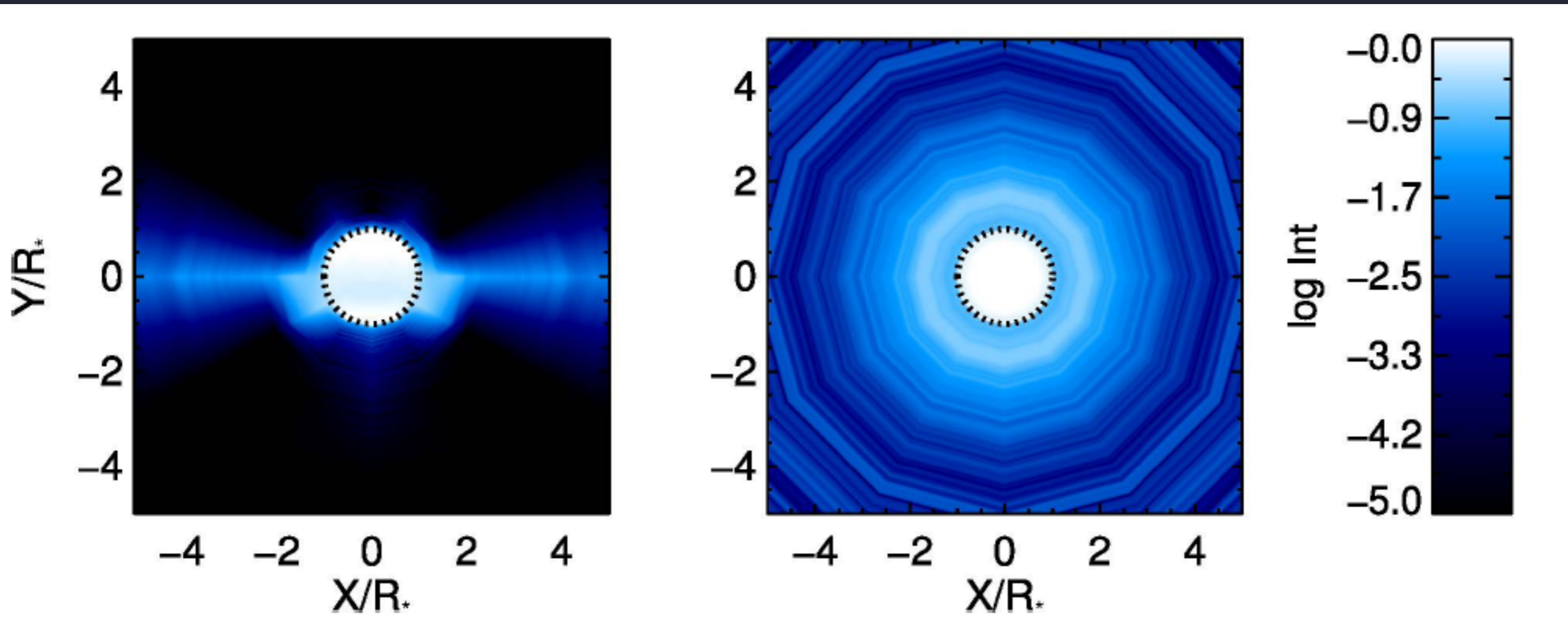
tilted dipole: oblique magnetic rotator



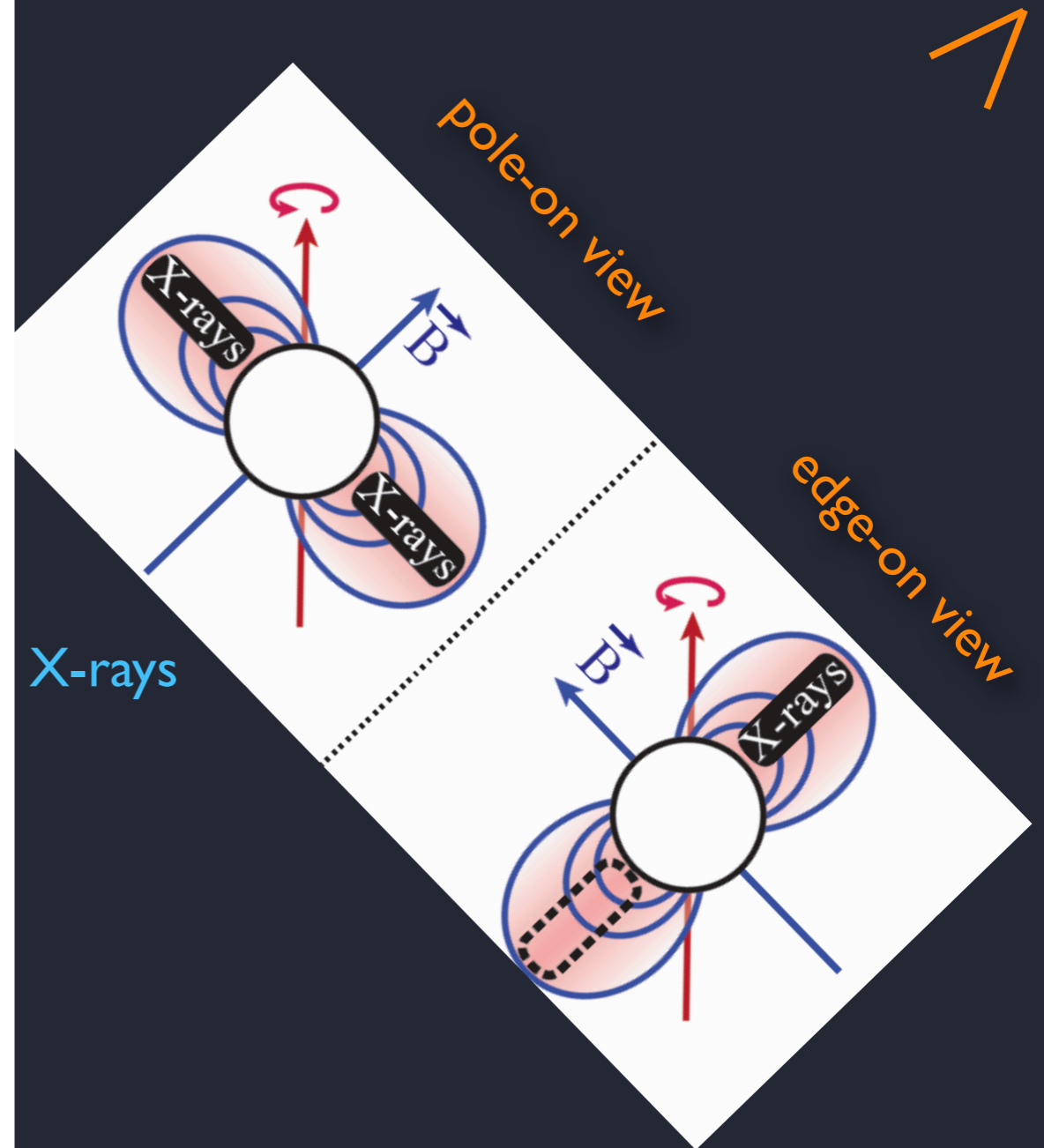
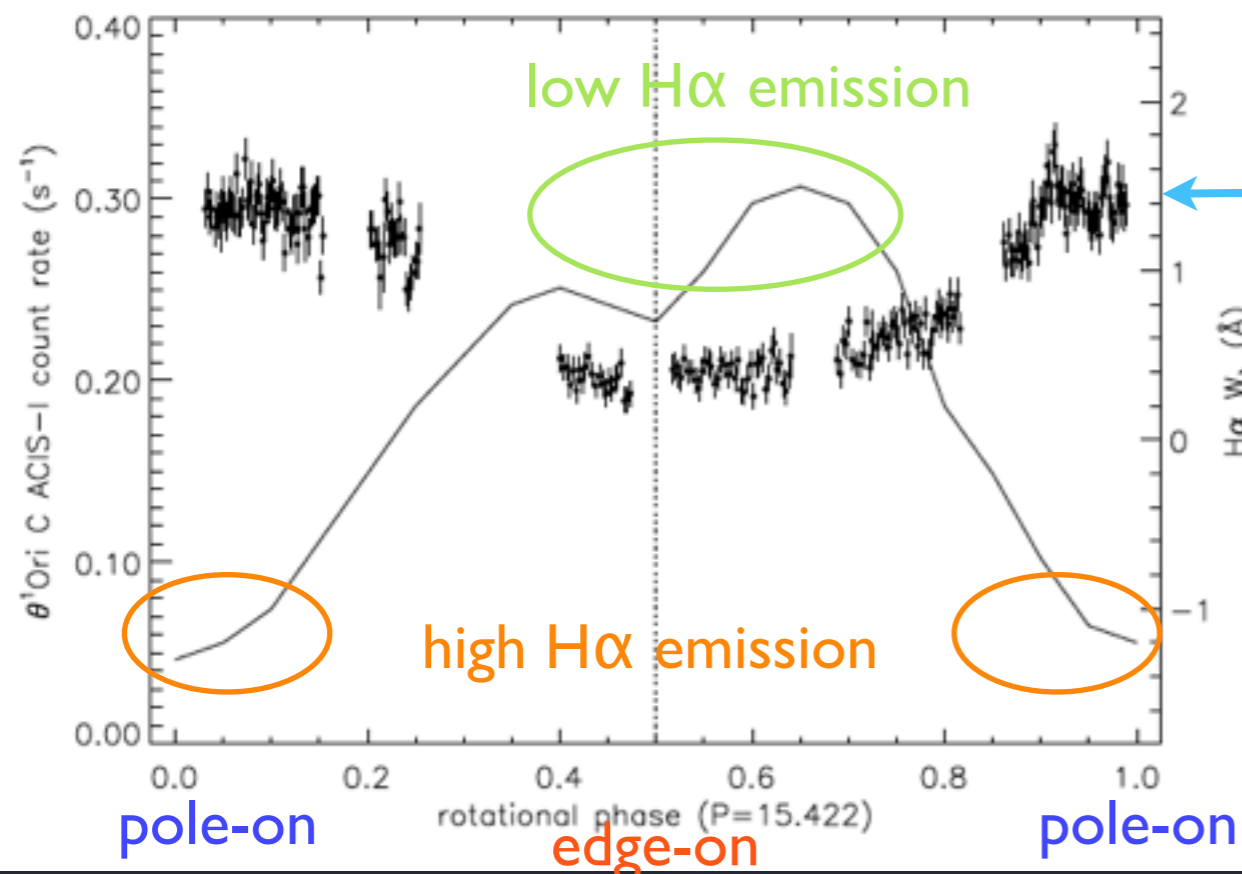
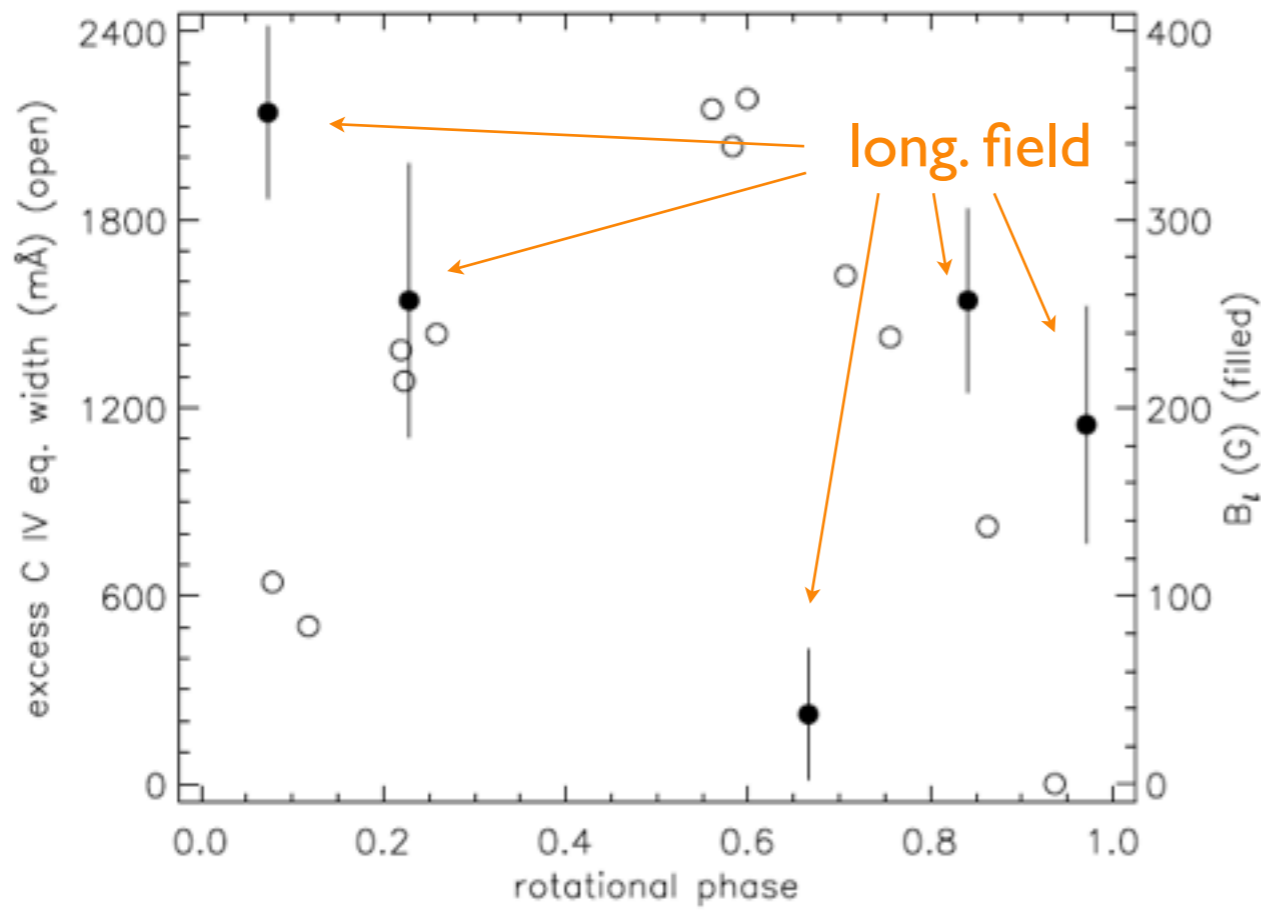
H α intensity map (ADM model)

edge-on: H α weaker

pole-on: H α stronger



tilted dipole: oblique magnetic rotator



MHD simulations: 2-D, hemispherical slice

density

temperature

X-ray emission

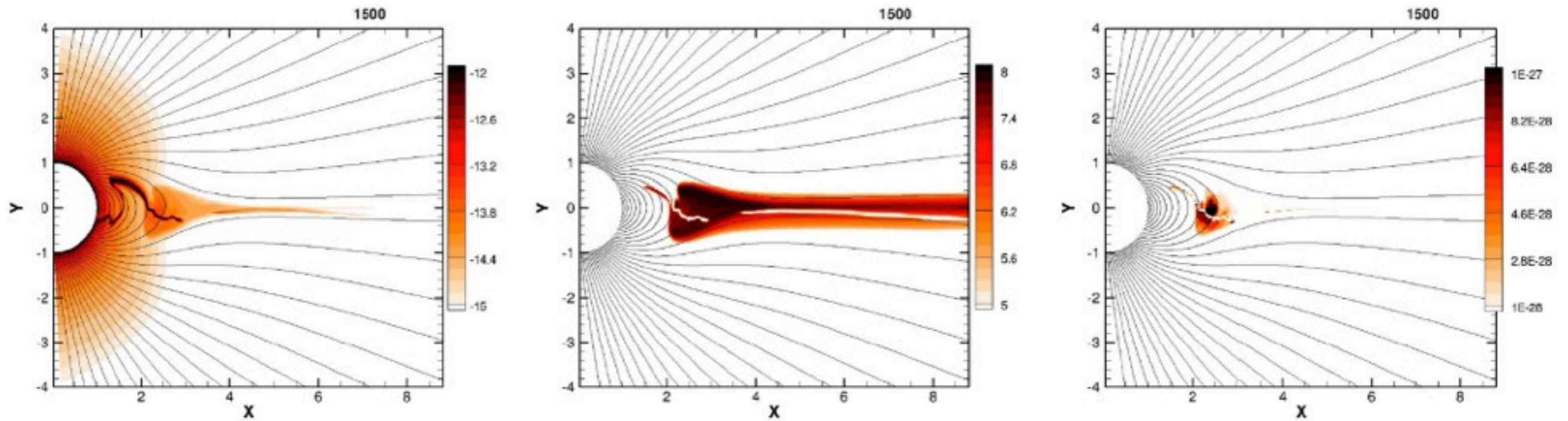
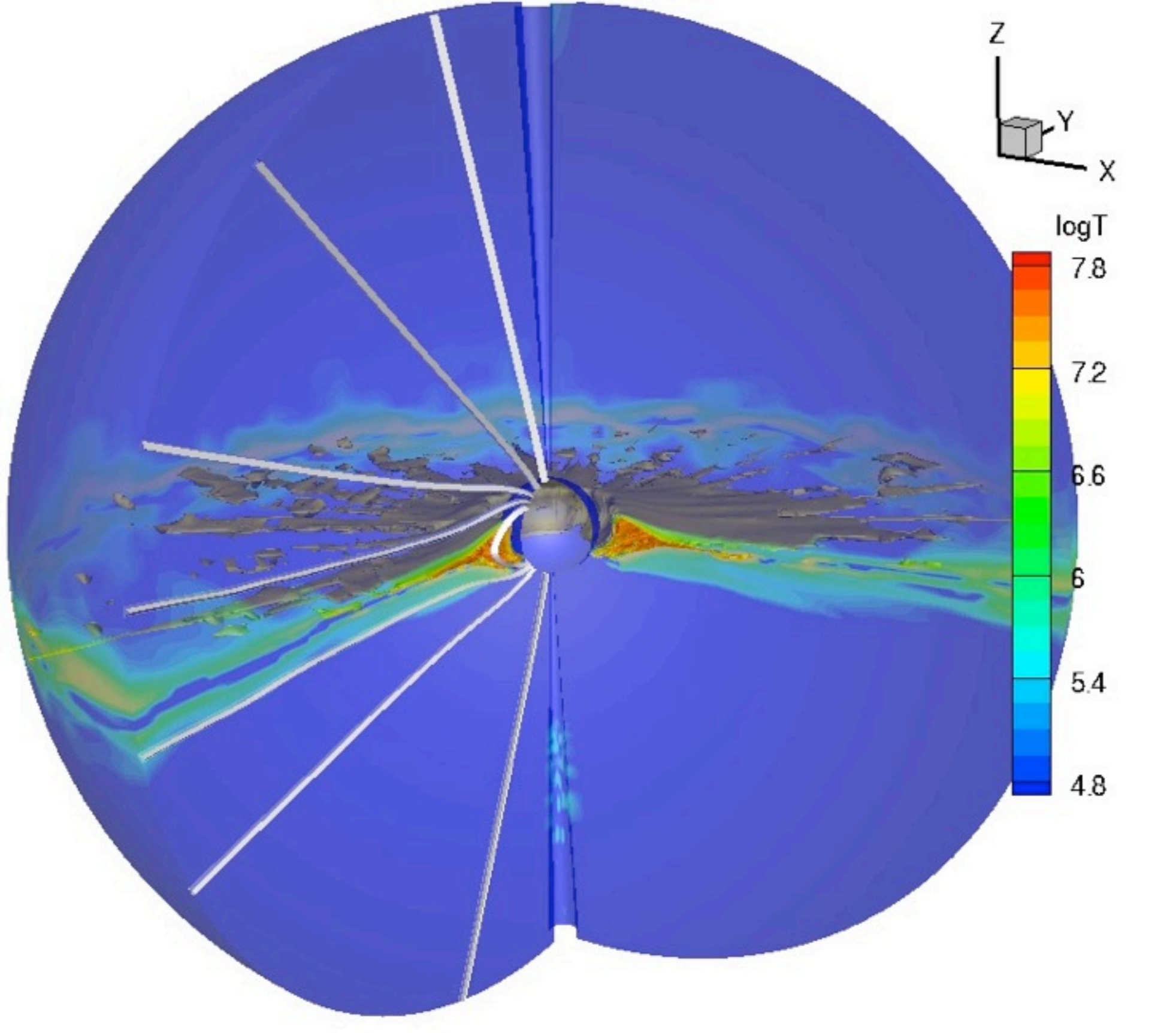


Figure 4. Colour plots of log density (left) and log temperature (middle) for arbitrary snapshot of structure in the standard model with $\eta_* = 100$ and no IC cooling. The right-hand panel plots the proxy X-ray emission XEM_{T_x} (weighted by the radius r) from (26), on a *linear* scale for a threshold X-ray temperature $T_x = 1.5$ MK.

ud-Doula et al. 2014

3-D MHD simulation: log Temperature



from A. ud-Doula

Chandra



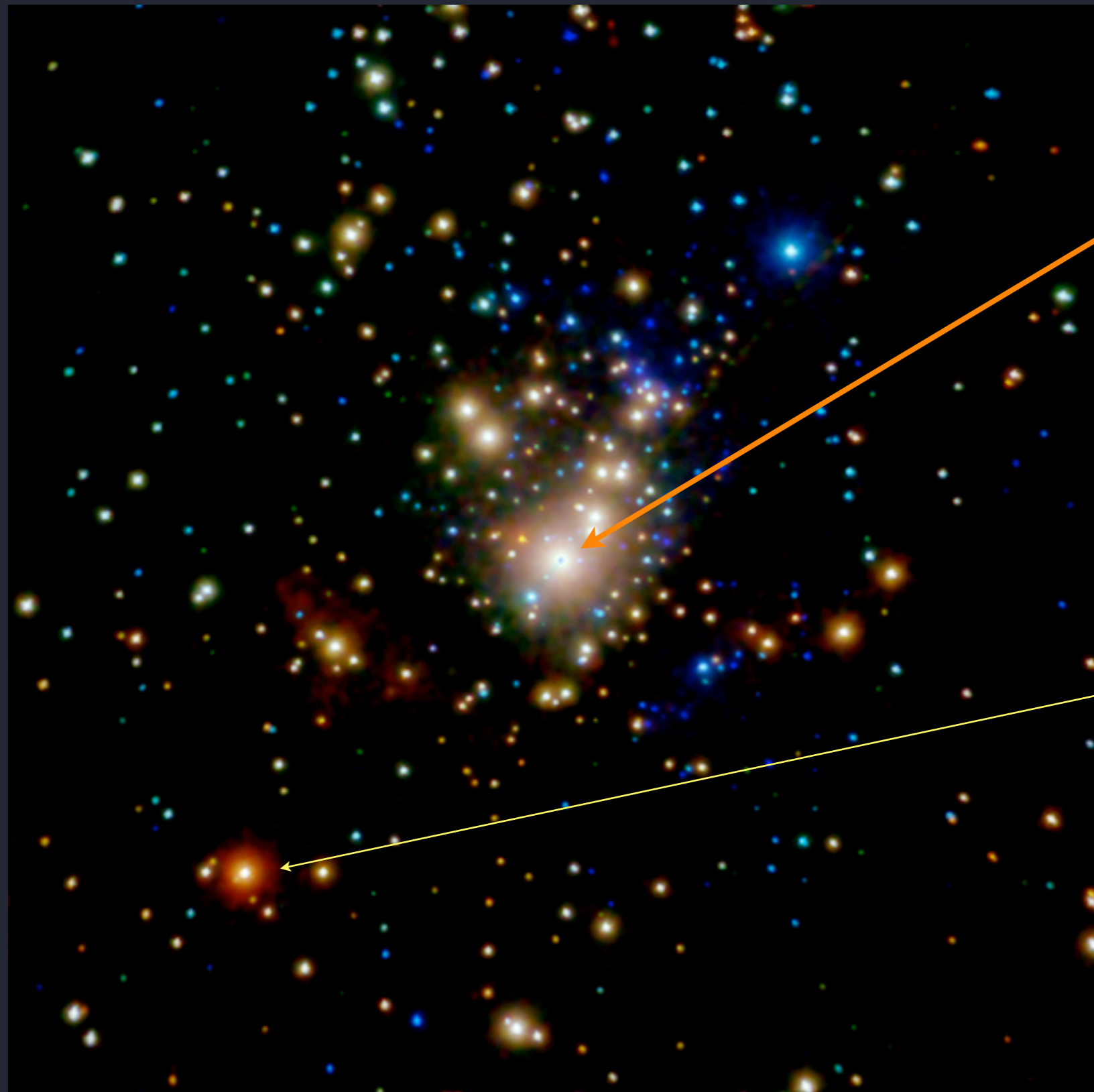
Orion Nebula Cluster - *Chandra*
color-coded by X-ray hardness

response to photons with $h\nu \sim 0.5 \text{ keV}$ up to a few keV
(corresp. $\sim 5\text{\AA}$ to 24\AA)

spectroscopy ($R < 1000$ corresp. $> 300 \text{ km/s}$)

small effective area (poor sensitivity)
but very low background and very well calibrated

$kT = h\nu$ gives
 $T \sim 12 \times 10^6 \text{ K}$
for 1 keV



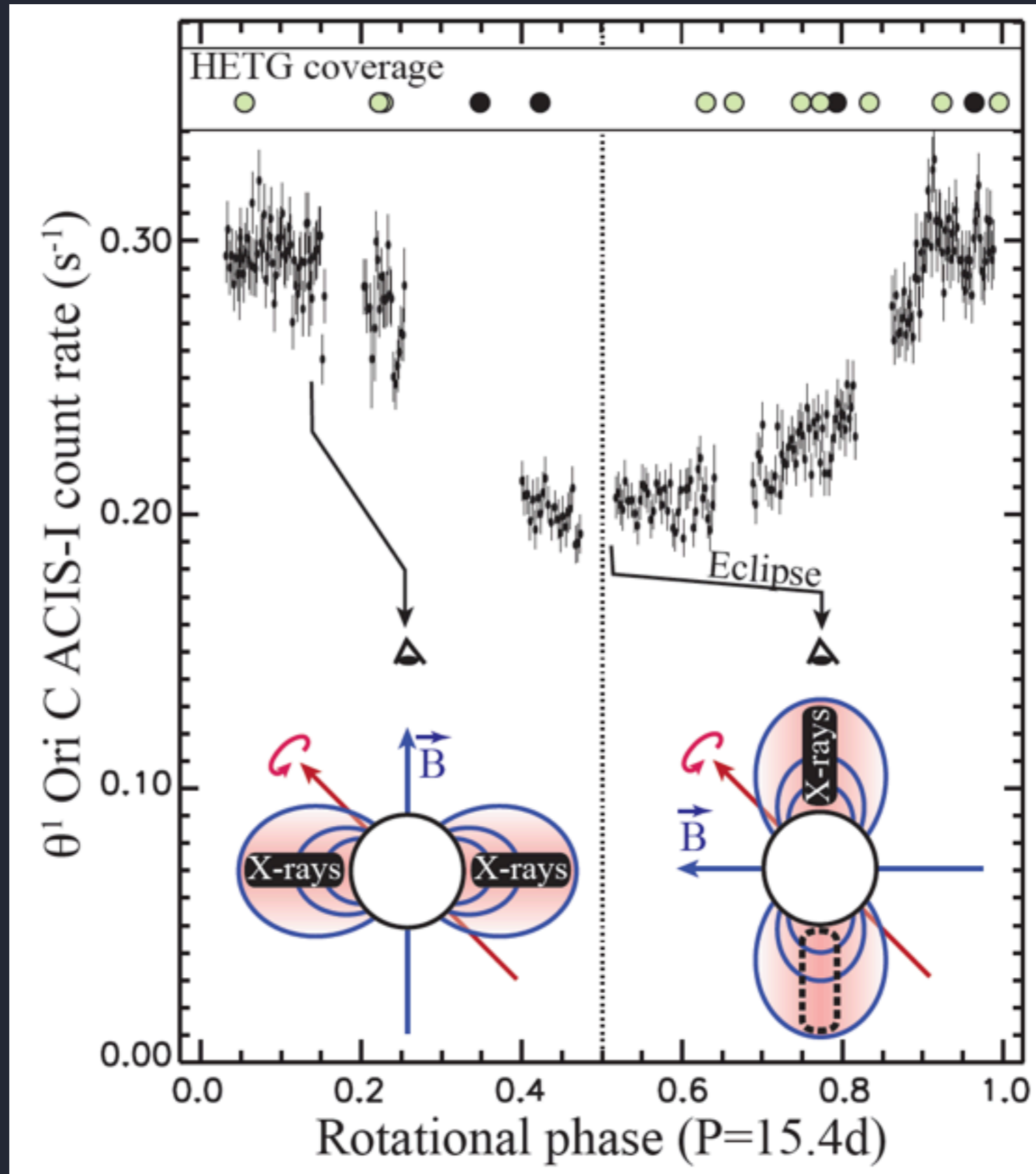
θ^1 Ori C:
strongest X-ray
source in the
cluster

θ^2 Ori A: non-
magnetic O star
with softer X-rays

Orion Nebula Cluster - *Chandra*
color-coded by X-ray hardness

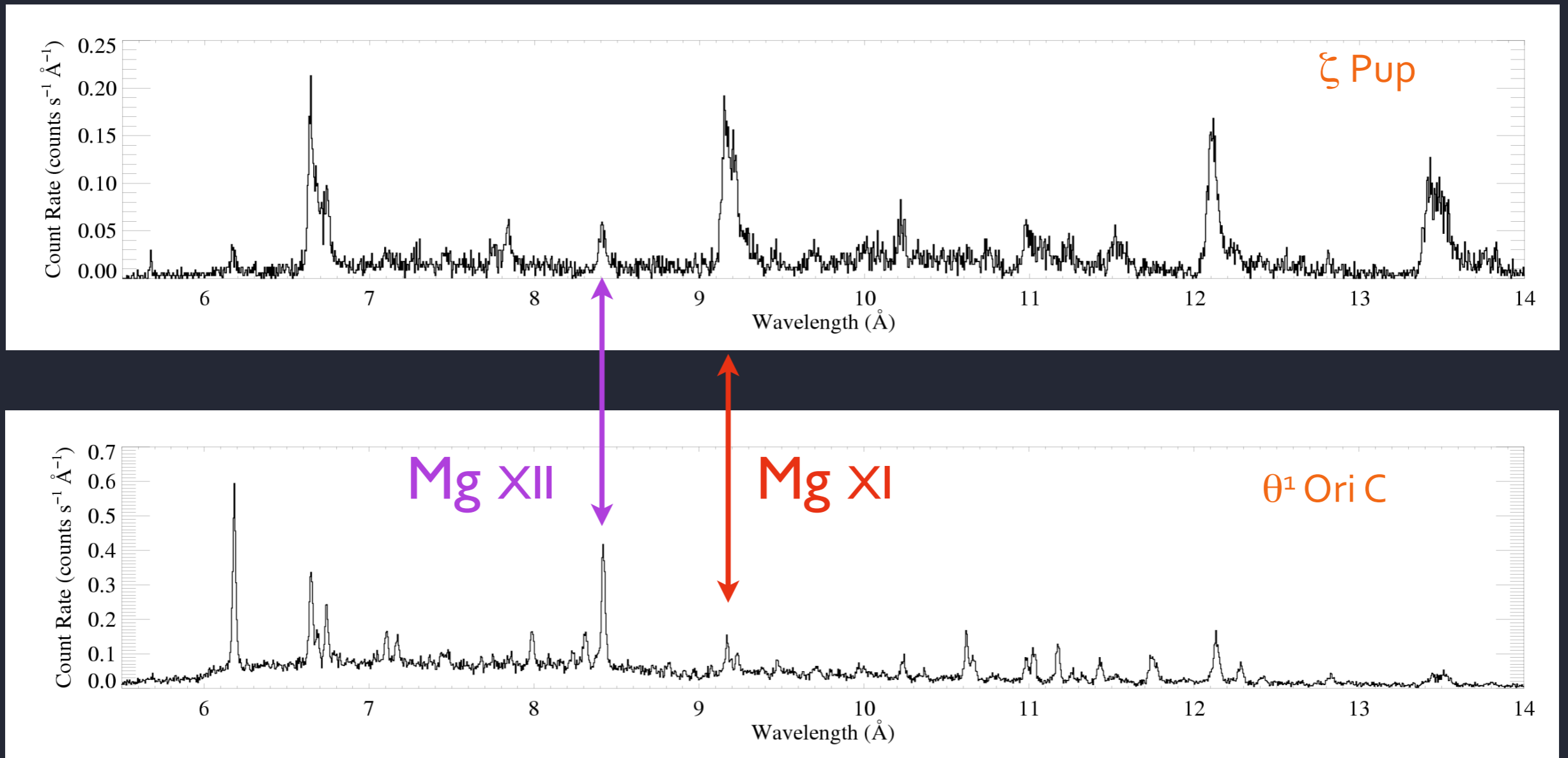


X-ray light curve: phase coverage: new data (11 new pointings to supplement 4 in Gagne et al. 2005)



Line ratios as temperature indicators

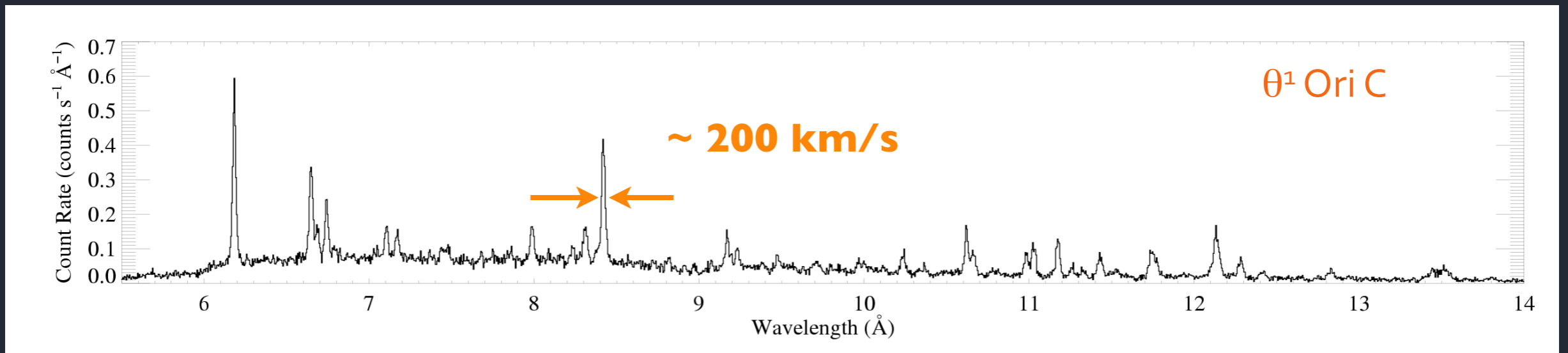
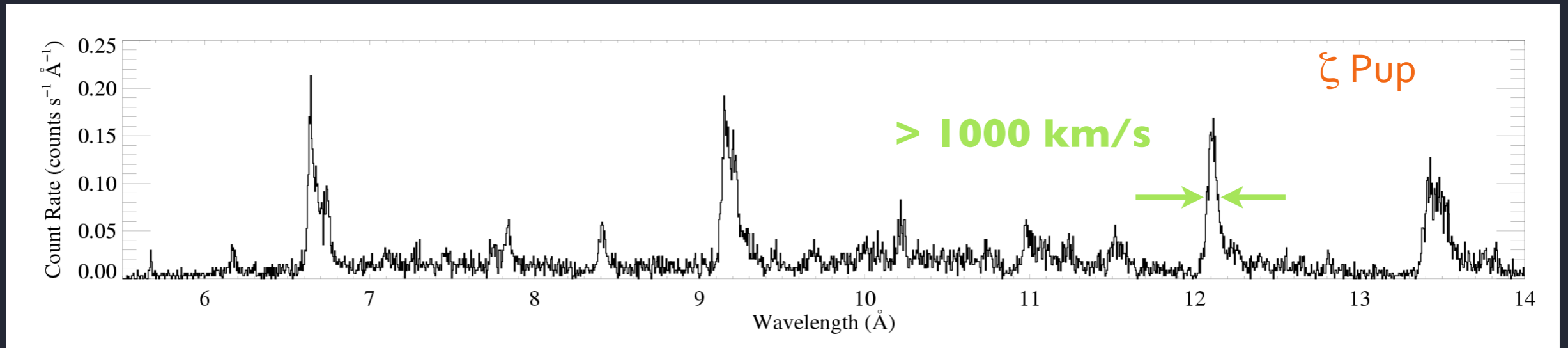
Mg XII / Mg XI is proportional to temperature



Chandra spectra of prototype non-magnetic (zeta Pup, top) and magnetic (θ^1 Ori C, bottom) stars

Line widths from gas kinematics

non-magnetic O stars: $v_{\text{line}} \sim v_{\text{wind}}$ but MCWS: $v_{\text{line}} < v_{\text{wind}}$



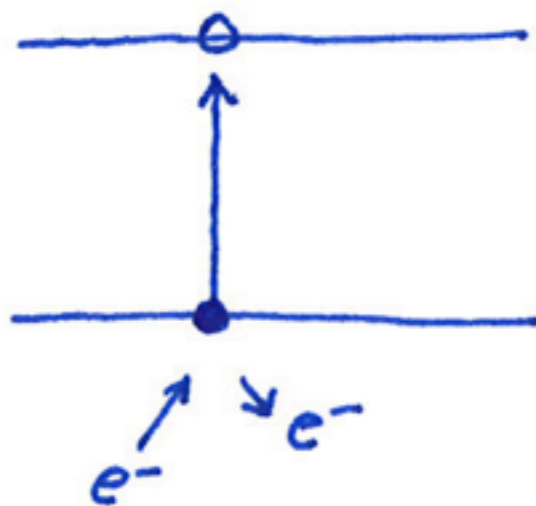
Chandra spectra of prototype non-magnetic (zeta Pup, top) and magnetic (θ^1 Ori C, bottom) stars

X-ray line emission process

thermal emission from collisional plasma

X-ray emission

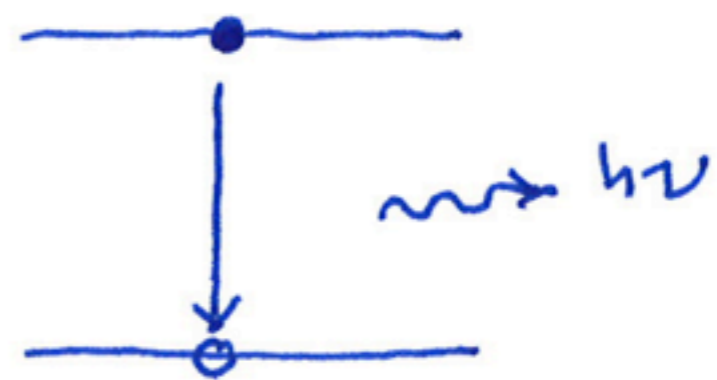
collisional
excitation



followed
by

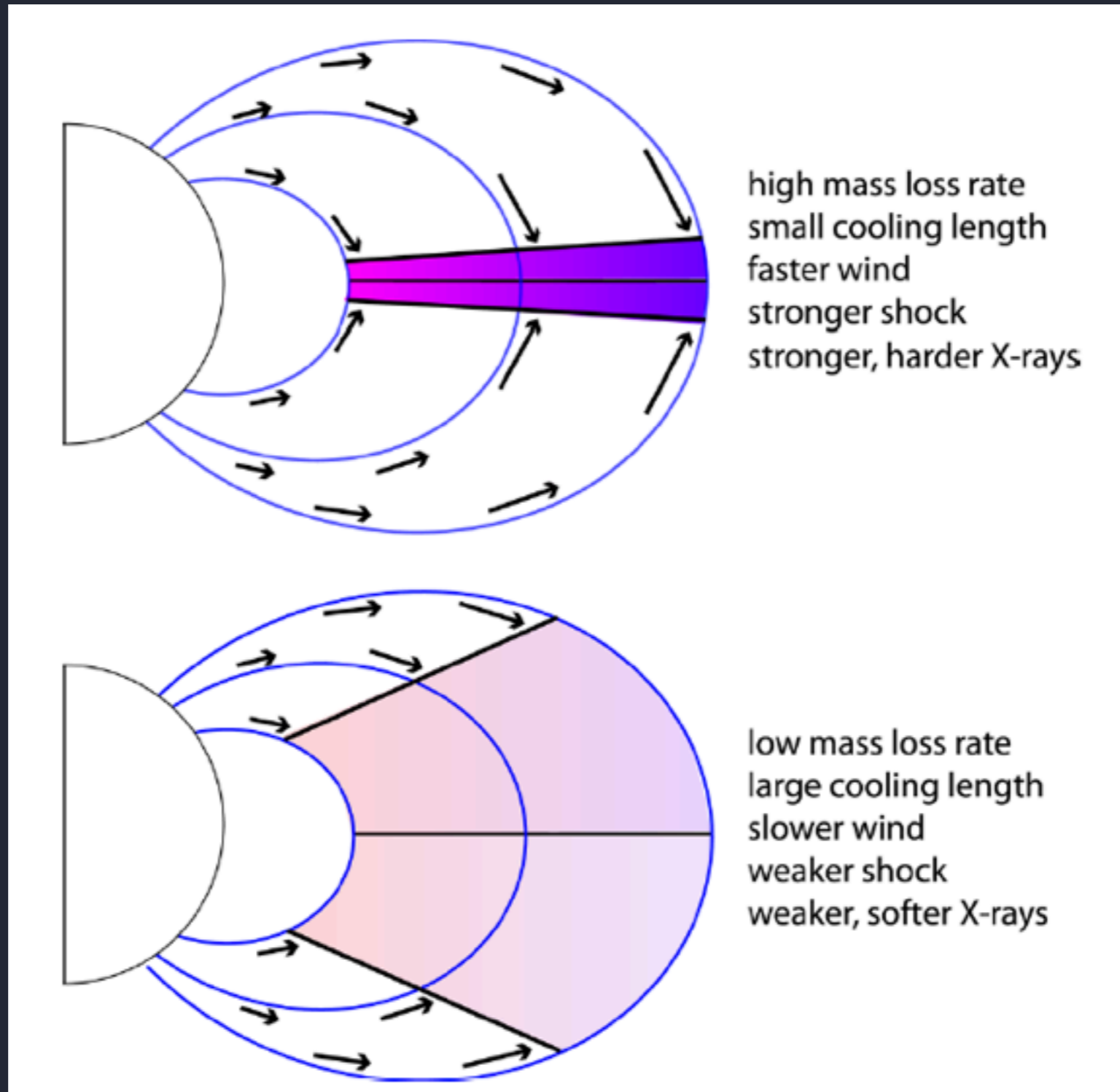


spontaneous
emission



Plasma heating from hydrodynamic shock

wind kinetic energy converted to heat: $T \sim 10^6 (v_{\text{shock}}/300 \text{ km/s})^2 \text{ K}$



from ud-Doula et al. 2014

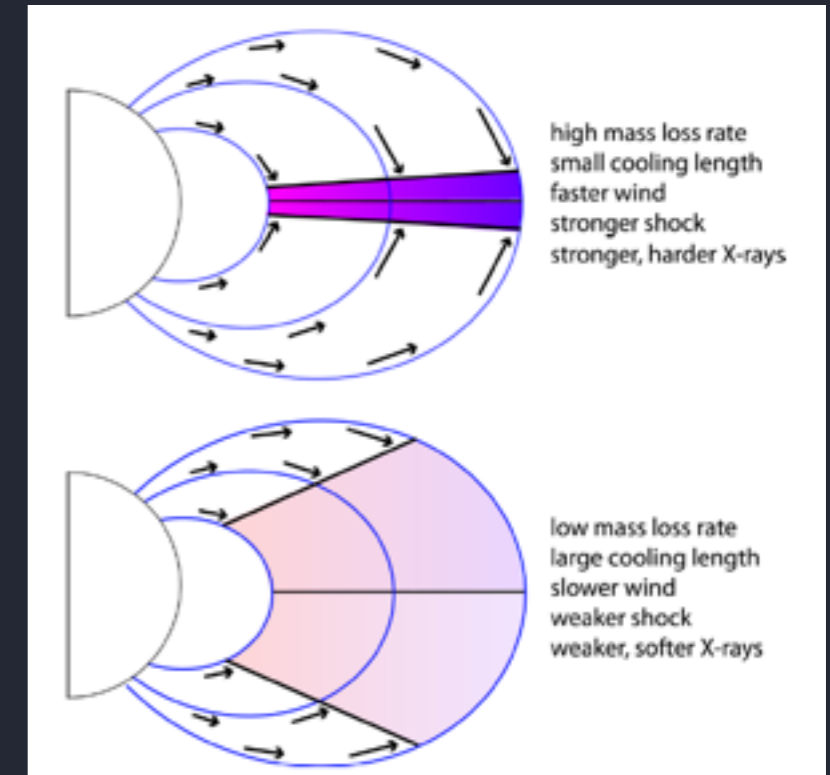
Overall level and hardness of X-ray emission

affected by:

amount of wind material fed into the magnetosphere

efficiency of shock heating (duty cycle of shock build up vs. fall-back/downflow)

specific kinetic energy: shock velocity (pre-shock wind velocity)

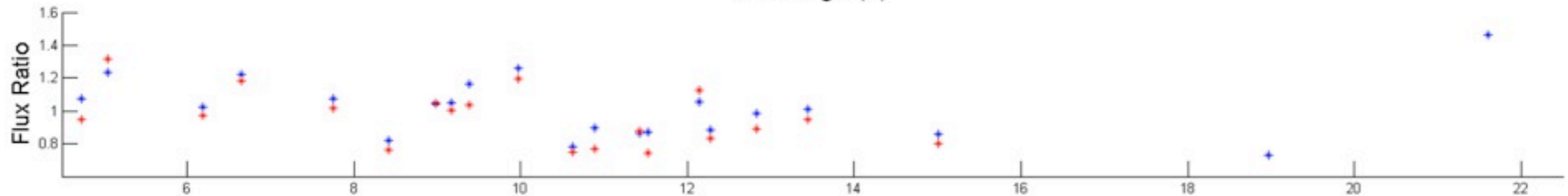
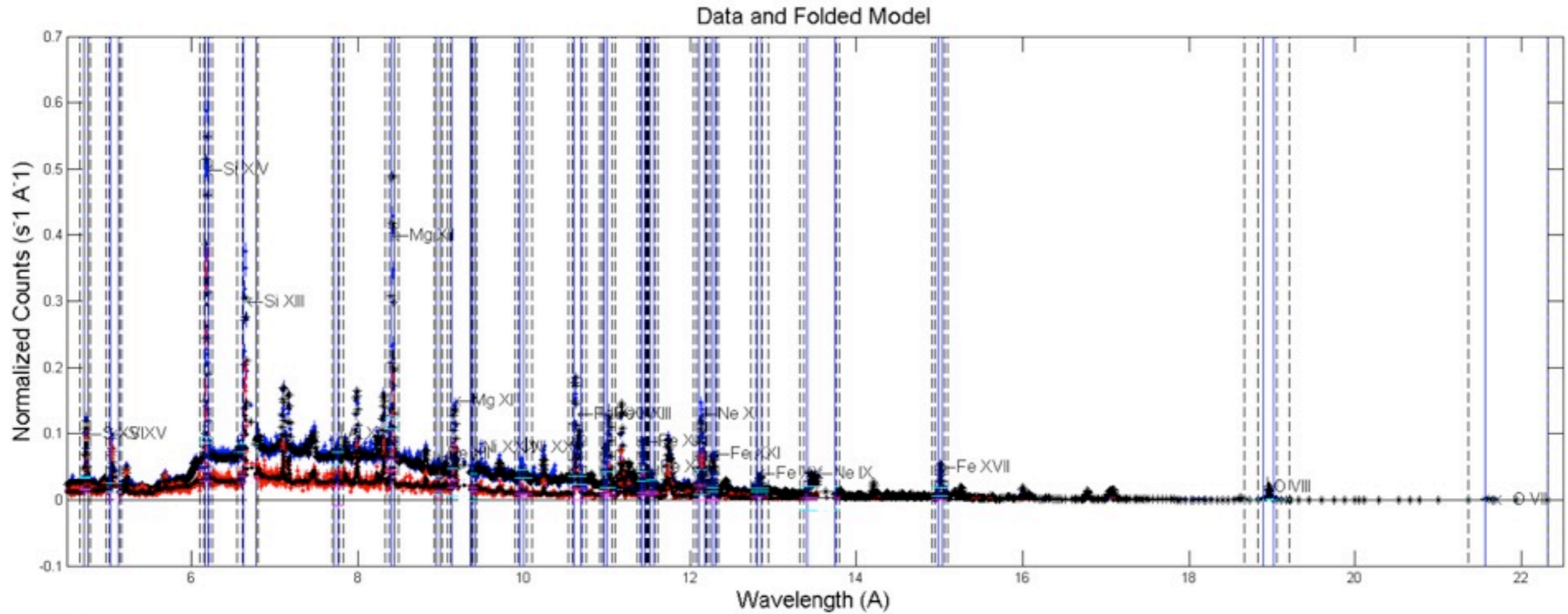


from ud-Doula et al. 2014

Goal: use the X-ray spectrum to measure the amount of hot plasma and its temperature distribution, compare results to simulations

Spectral modeling: coadded 15 observations

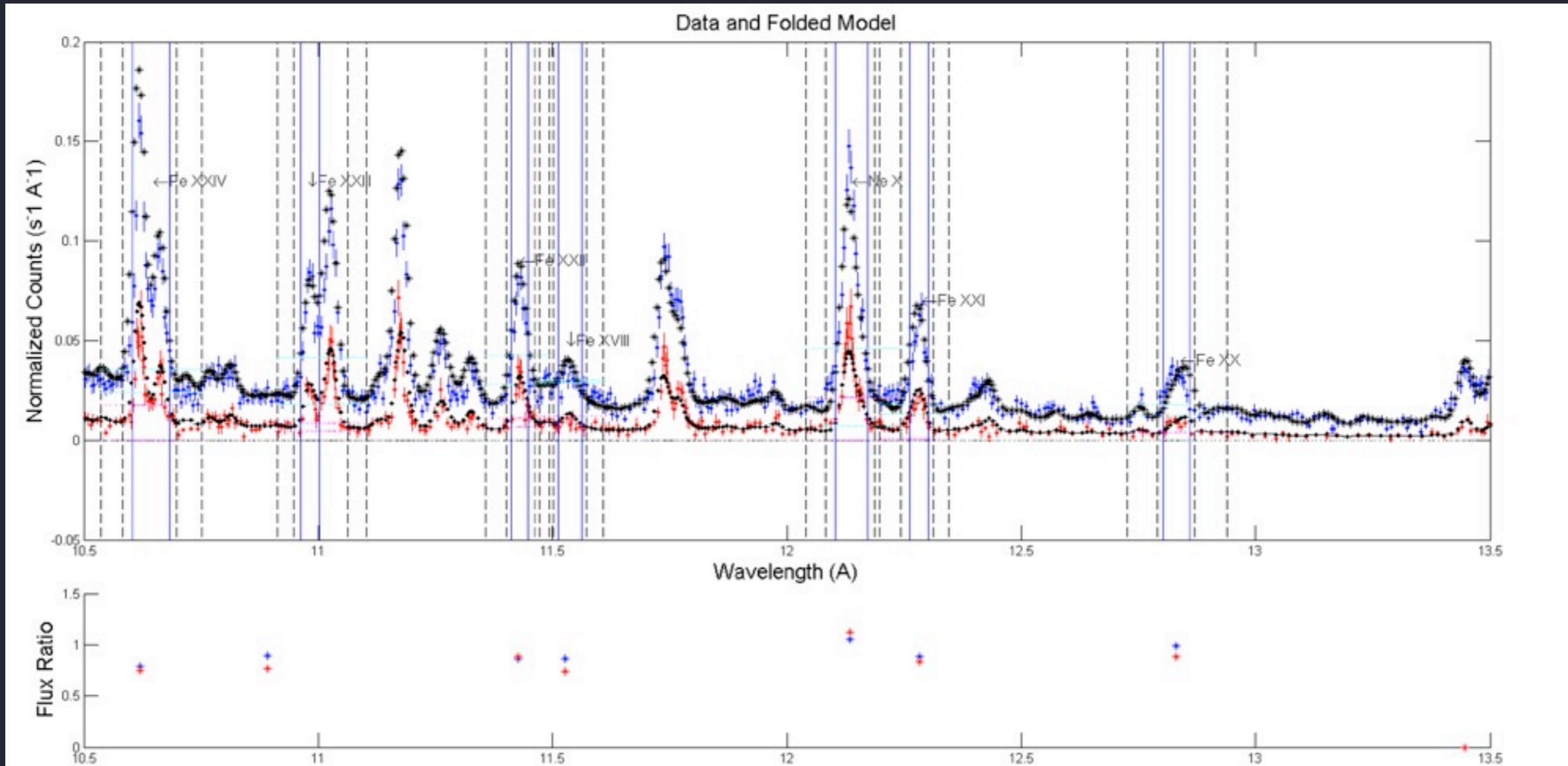
collisional-radiative equilibrium model (APEC): temperature and emission measure are free parameters, along with line widths and (potentially) abundances



fit to *Chandra* spectrum

Spectral modeling

zoom-in: black = model; red, blue = data (two grating arrays on *Chandra* produce two spectra, simultaneously)



fit to *Chandra* spectrum

data - model agreement is quite good

Spectral modeling

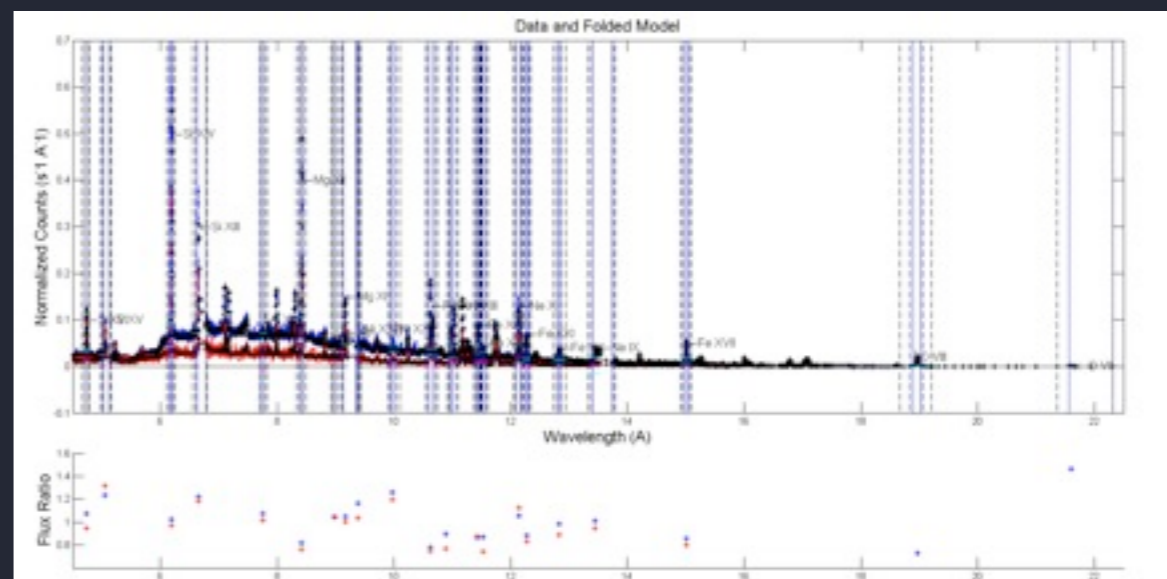
work presented here is preliminary

best-fit model parameters: temperature distribution in the plasma, line widths, absorption

```
=====
Model (bapec<1> + bapec<2> + bapec<3> + bapec<4> + bapec<5> + bapec<6>)TBabs<7>
Source No.: 1 Active/On
Model Model Component Parameter Unit Value
par comp
  1 1 bapec kT keV 0.200000 frozen
  2 1 bapec Abundanc 1.00000 frozen
  3 1 bapec Redshift 0.0 frozen
  4 1 bapec Velocity km/s 290.281 +/- 2.52376
  5 1 bapec norm 1.11264E-02 +/- 5.74059E-04
  6 2 bapec kT keV 0.400000 frozen
  7 2 bapec Abundanc 1.00000 frozen
  8 2 bapec Redshift 0.0 frozen
  9 2 bapec Velocity km/s 290.281 = 1.0*4
 10 2 bapec norm 2.00501E-03 +/- 1.13754E-04
 11 3 bapec kT keV 0.800000 frozen
 12 3 bapec Abundanc 1.00000 frozen
 13 3 bapec Redshift 0.0 frozen
 14 3 bapec Velocity km/s 290.281 = 1.0*4
 15 3 bapec norm 5.02117E-03 +/- 9.06196E-05
 16 4 bapec kT keV 1.60000 frozen
 17 4 bapec Abundanc 1.00000 frozen
 18 4 bapec Redshift 0.0 frozen
 19 4 bapec Velocity km/s 290.281 = 1.0*4
 20 4 bapec norm 7.56200E-03 +/- 1.89407E-04
 21 5 bapec kT keV 3.20000 frozen
 22 5 bapec Abundanc 1.00000 frozen
 23 5 bapec Redshift 0.0 frozen
 24 5 bapec Velocity km/s 290.281 = 1.0*4
 25 5 bapec norm 2.07156E-02 +/- 4.52703E-04
 26 6 bapec kT keV 6.40000 frozen
 27 6 bapec Abundanc 1.00000 frozen
 28 6 bapec Redshift 0.0 frozen
 29 6 bapec Velocity km/s 290.281 = 1.0*4
 30 6 bapec norm 2.45517E-03 +/- 3.00636E-04
 31 7 TBabs nH 10^22 0.616796 +/- 4.19245E-03
=====

Fit statistic : C-Statistic = 13812.32 using 4807 PHA bins and 4799 degrees of freedom.
Warning: cstat statistic is only valid for Poisson data.
Source file is not Poisson

Test statistic : Chi-Squared = 9258.43 using 4807 PHA bins.
Reduced chi-squared = 1.92924 for 4799 degrees of freedom
Null hypothesis probability = 2.369129e-286
```



fit to Chandra spectrum

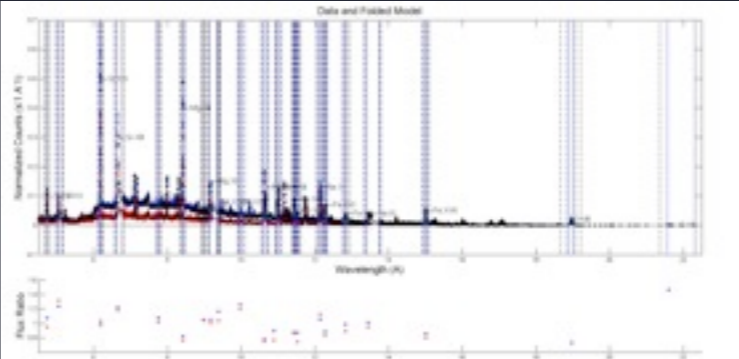
line widths ~ 300 km/s

ISM column density ~ $6 \times 10^{21} \text{ cm}^{-2}$
(maybe a bit more than ISM)

Spectral modeling

temperature distribution

from the APEC spectral fit

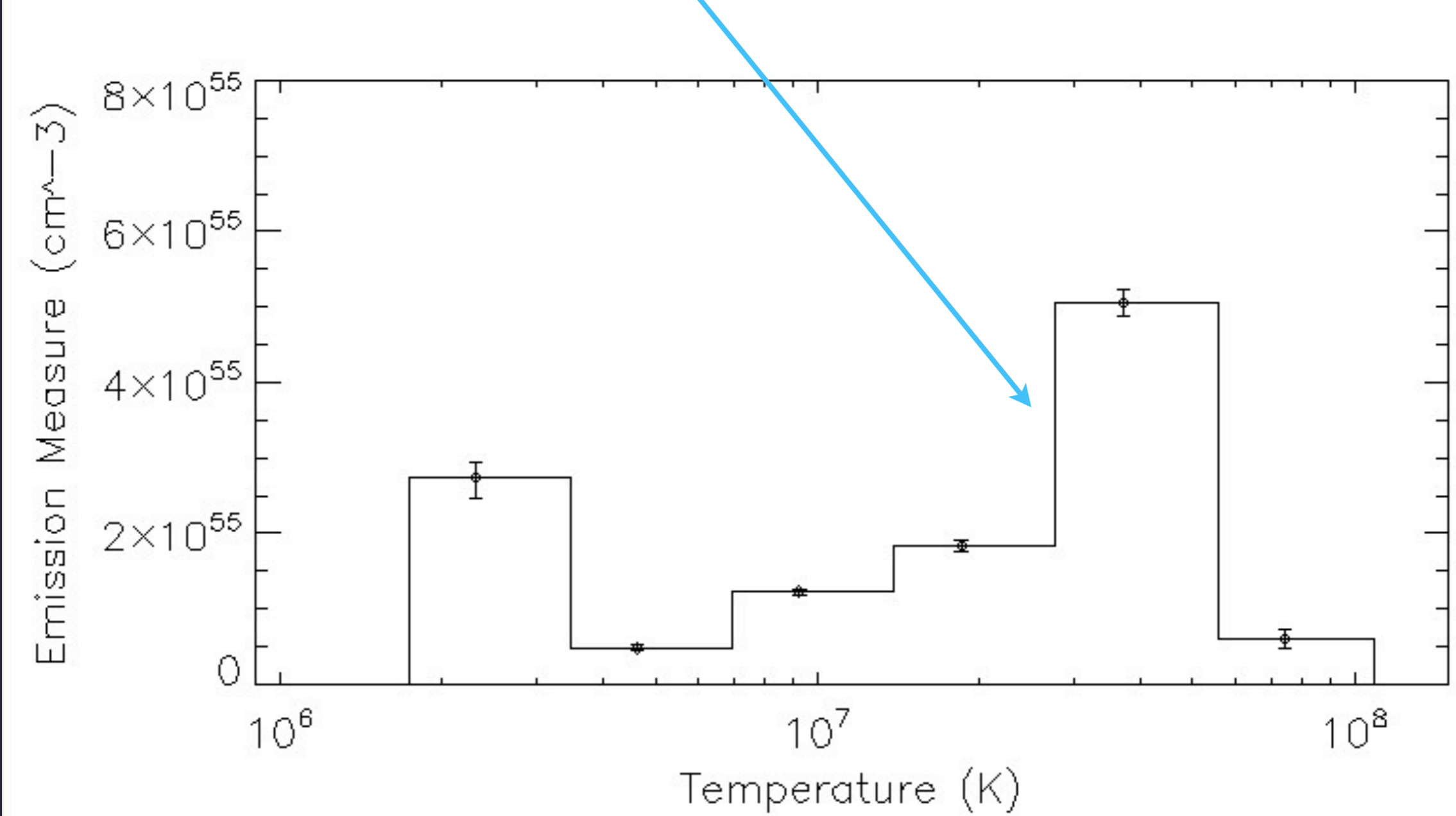


fit to *Chandra* spectrum

Table 1: Summary of fit parameters

| Comp | Group | Parameter | Unit | Value |
|------|-------|-----------|---------|---------|
| 1 | 1 | Norm | 1.0 | 1.00000 |
| 1 | 1 | Redshift | | 0.00000 |
| 1 | 1 | Velocity | km/s | 0.00000 |
| 2 | 2 | Norm | 0.20000 | 0.20000 |
| 2 | 2 | Redshift | | 0.00000 |
| 2 | 2 | Velocity | km/s | 0.00000 |
| 3 | 3 | Norm | 0.10000 | 0.10000 |
| 3 | 3 | Redshift | | 0.00000 |
| 3 | 3 | Velocity | km/s | 0.00000 |
| 4 | 4 | Norm | 0.05000 | 0.05000 |
| 4 | 4 | Redshift | | 0.00000 |
| 4 | 4 | Velocity | km/s | 0.00000 |
| 5 | 5 | Norm | 0.02000 | 0.02000 |
| 5 | 5 | Redshift | | 0.00000 |
| 5 | 5 | Velocity | km/s | 0.00000 |
| 6 | 6 | Norm | 0.01000 | 0.01000 |
| 6 | 6 | Redshift | | 0.00000 |
| 6 | 6 | Velocity | km/s | 0.00000 |
| 7 | 7 | Norm | 0.00500 | 0.00500 |
| 7 | 7 | Redshift | | 0.00000 |
| 7 | 7 | Velocity | km/s | 0.00000 |
| 8 | 8 | Norm | 0.00200 | 0.00200 |
| 8 | 8 | Redshift | | 0.00000 |
| 8 | 8 | Velocity | km/s | 0.00000 |
| 9 | 9 | Norm | 0.00100 | 0.00100 |
| 9 | 9 | Redshift | | 0.00000 |
| 9 | 9 | Velocity | km/s | 0.00000 |
| 10 | 10 | Norm | 0.00050 | 0.00050 |
| 10 | 10 | Redshift | | 0.00000 |
| 10 | 10 | Velocity | km/s | 0.00000 |
| 11 | 11 | Norm | 0.00020 | 0.00020 |
| 11 | 11 | Redshift | | 0.00000 |
| 11 | 11 | Velocity | km/s | 0.00000 |
| 12 | 12 | Norm | 0.00010 | 0.00010 |
| 12 | 12 | Redshift | | 0.00000 |
| 12 | 12 | Velocity | km/s | 0.00000 |
| 13 | 13 | Norm | 0.00005 | 0.00005 |
| 13 | 13 | Redshift | | 0.00000 |
| 13 | 13 | Velocity | km/s | 0.00000 |
| 14 | 14 | Norm | 0.00002 | 0.00002 |
| 14 | 14 | Redshift | | 0.00000 |
| 14 | 14 | Velocity | km/s | 0.00000 |
| 15 | 15 | Norm | 0.00001 | 0.00001 |
| 15 | 15 | Redshift | | 0.00000 |
| 15 | 15 | Velocity | km/s | 0.00000 |
| 16 | 16 | Norm | 0.00000 | 0.00000 |
| 16 | 16 | Redshift | | 0.00000 |
| 16 | 16 | Velocity | km/s | 0.00000 |
| 17 | 17 | Norm | 0.00000 | 0.00000 |
| 17 | 17 | Redshift | | 0.00000 |
| 17 | 17 | Velocity | km/s | 0.00000 |
| 18 | 18 | Norm | 0.00000 | 0.00000 |
| 18 | 18 | Redshift | | 0.00000 |
| 18 | 18 | Velocity | km/s | 0.00000 |
| 19 | 19 | Norm | 0.00000 | 0.00000 |
| 19 | 19 | Redshift | | 0.00000 |
| 19 | 19 | Velocity | km/s | 0.00000 |
| 20 | 20 | Norm | 0.00000 | 0.00000 |
| 20 | 20 | Redshift | | 0.00000 |
| 20 | 20 | Velocity | km/s | 0.00000 |
| 21 | 21 | Norm | 0.00000 | 0.00000 |
| 21 | 21 | Redshift | | 0.00000 |
| 21 | 21 | Velocity | km/s | 0.00000 |
| 22 | 22 | Norm | 0.00000 | 0.00000 |
| 22 | 22 | Redshift | | 0.00000 |
| 22 | 22 | Velocity | km/s | 0.00000 |

Chi-Square statistic: $\chi^2 = 282.02$ using 497 PH bins and 478 degrees of freedom.
Reduced chi-square: 0.58754



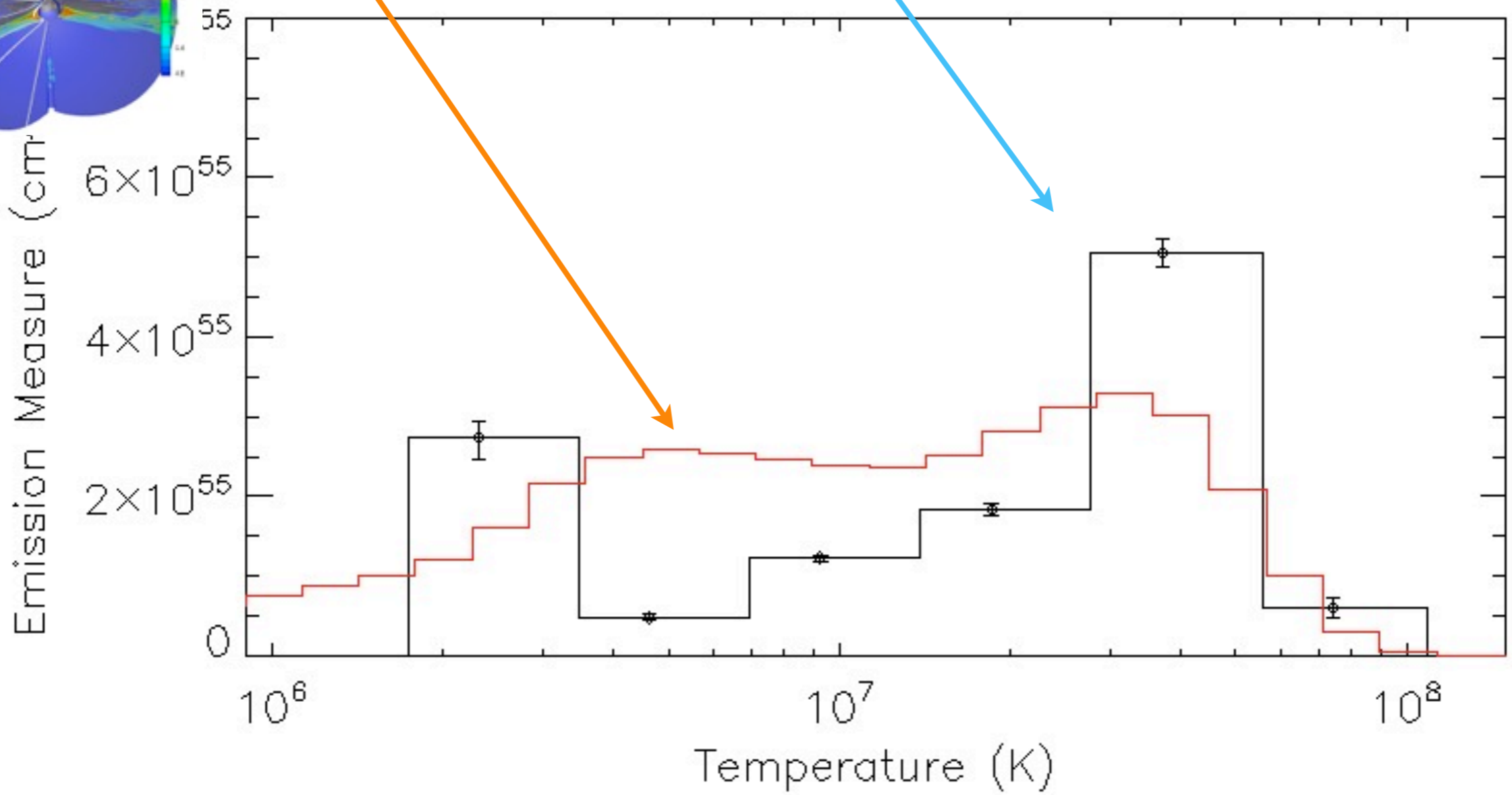
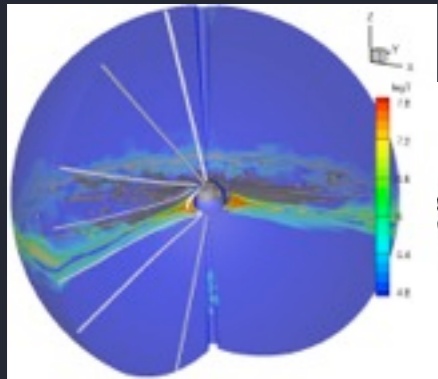
Spectral modeling

The overall amount of hot plasma produced in the MHD simulations is in excellent agreement with the data; the temperature distribution is in good agreement, too.

Emission Measure (EM) distribution

from 3-D MHD simulation

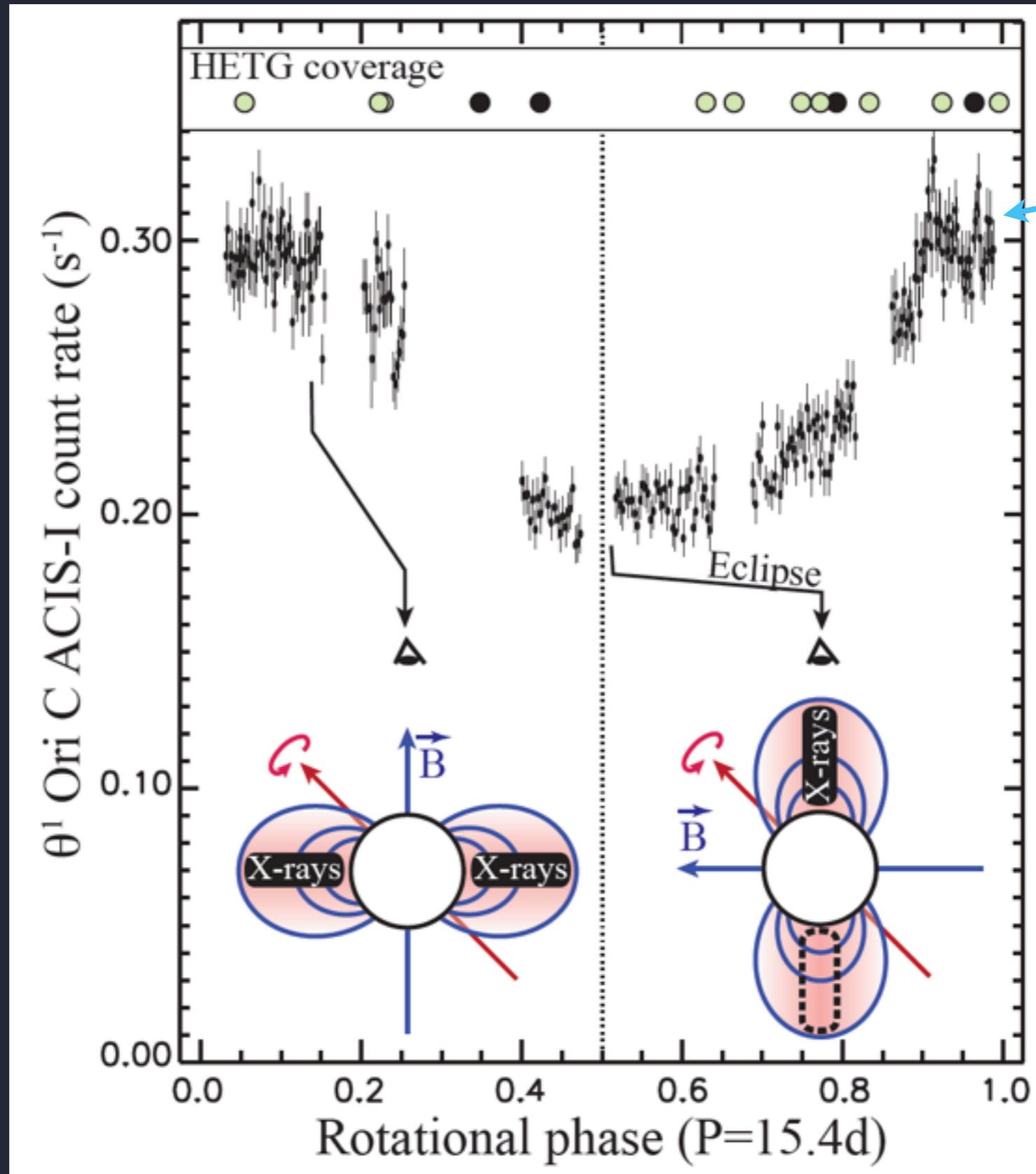
APEC spectral fit



rotationally modulated X-ray variability

X-ray light curve: phase coverage: new data (11 new pointings to supplement 4 in Gagne et al. 2005)

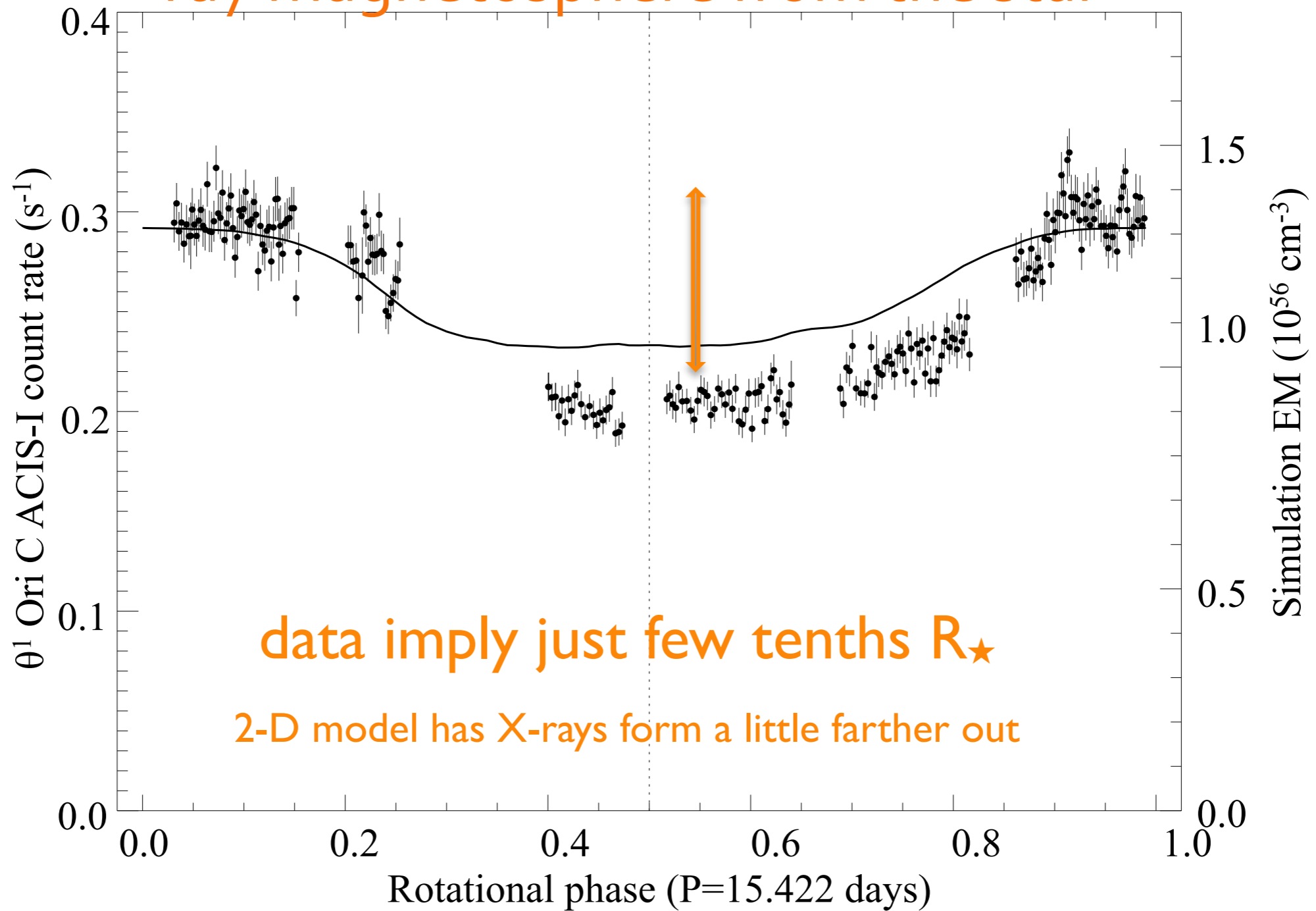
work presented here is preliminary



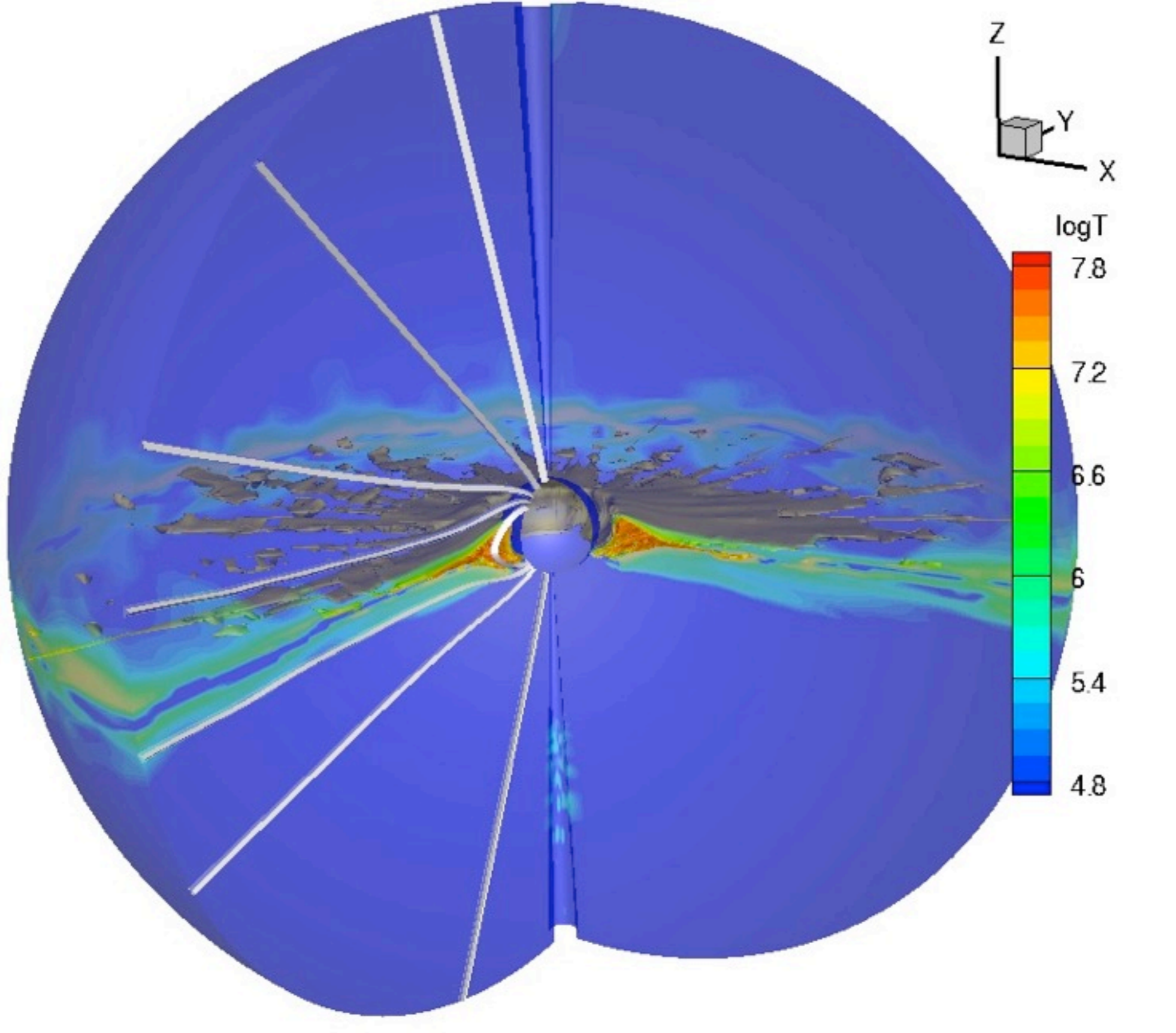
X-rays: occultation causes the magnetospheric eclipse

Location of hot plasma from eclipse depth: *occultation*

Eclipse depth depends on distance of X-ray magnetosphere from the star

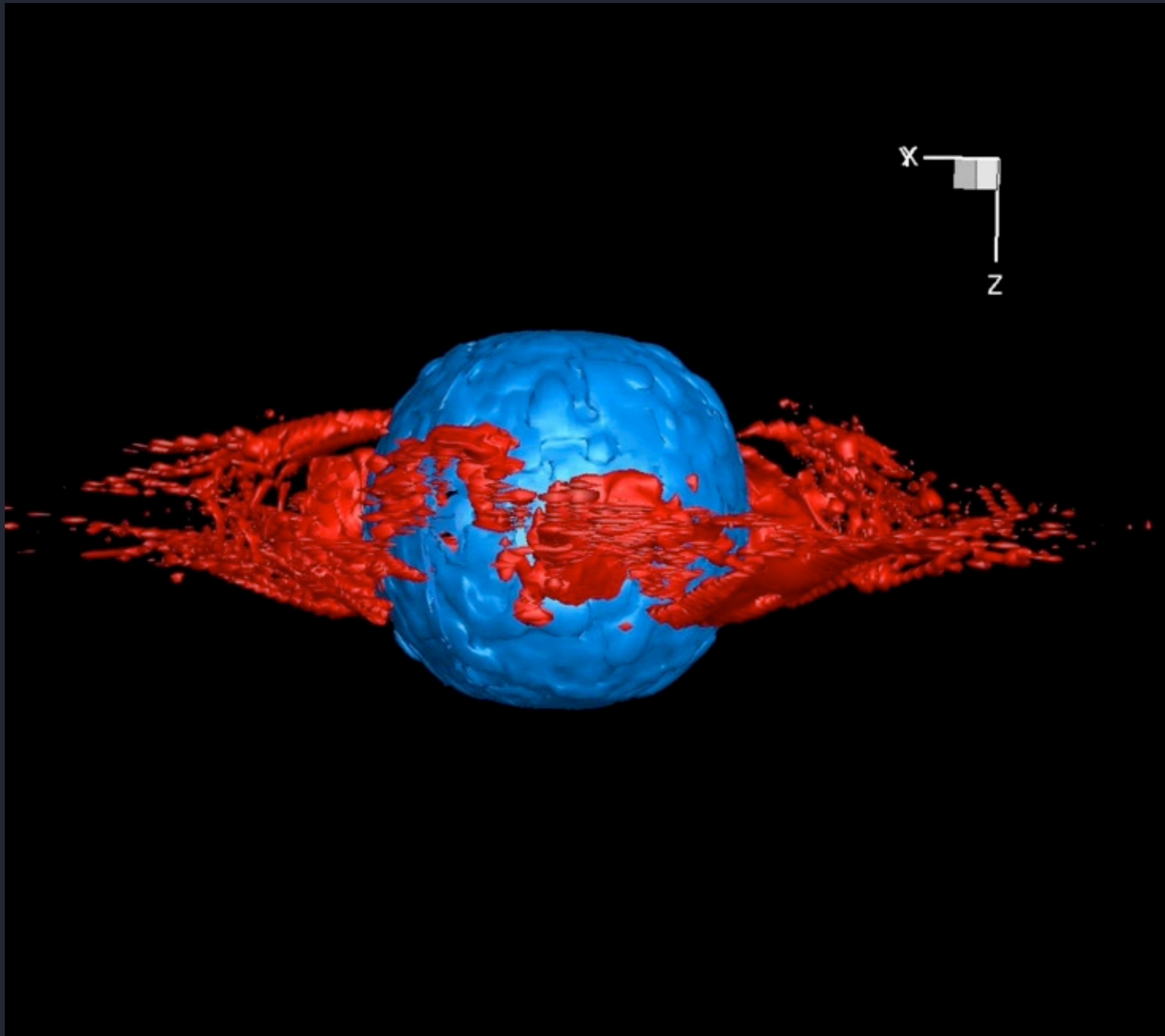


3-D MHD simulation: what about 3-D?



from A. ud-Doula

3-D MHD simulation: what about 3-D?



from A. ud-Doula

3-D MHD simulation: what about absorption?

optical depth - in ADM model

Analytic Dynamical Magnetosphere 7

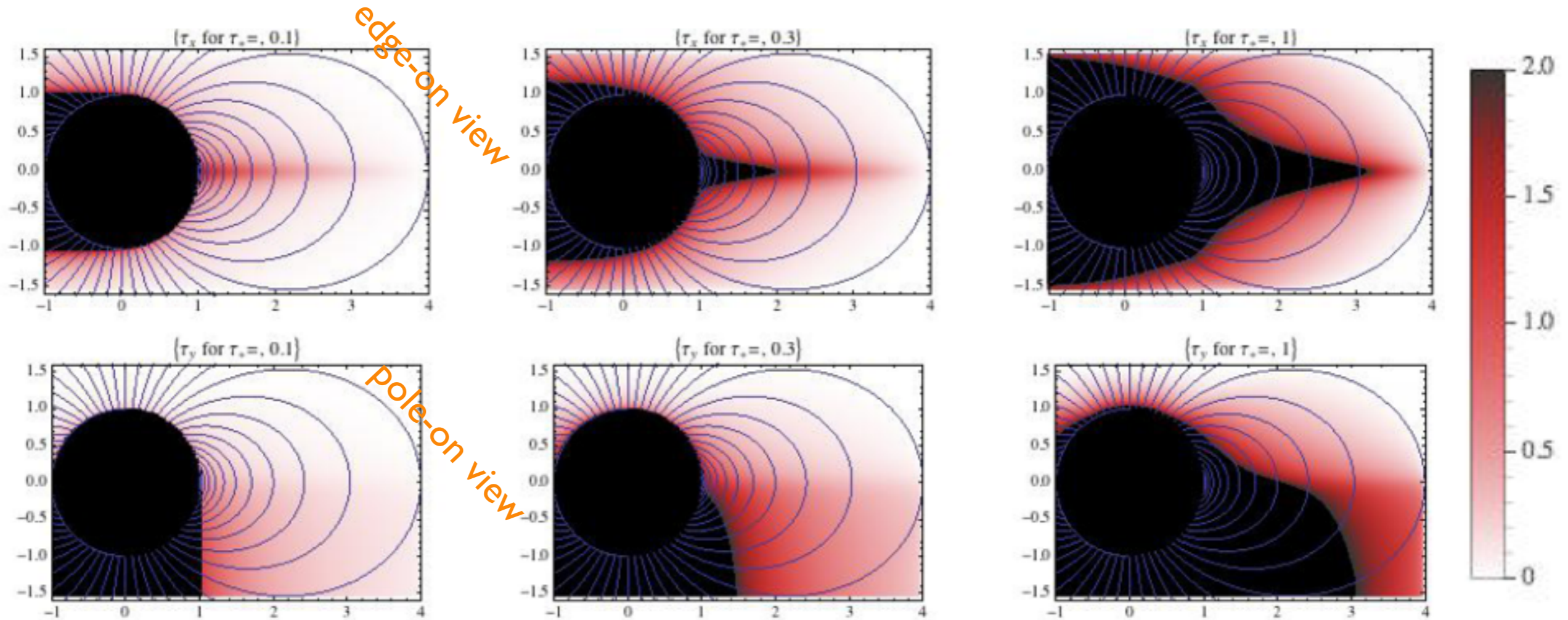
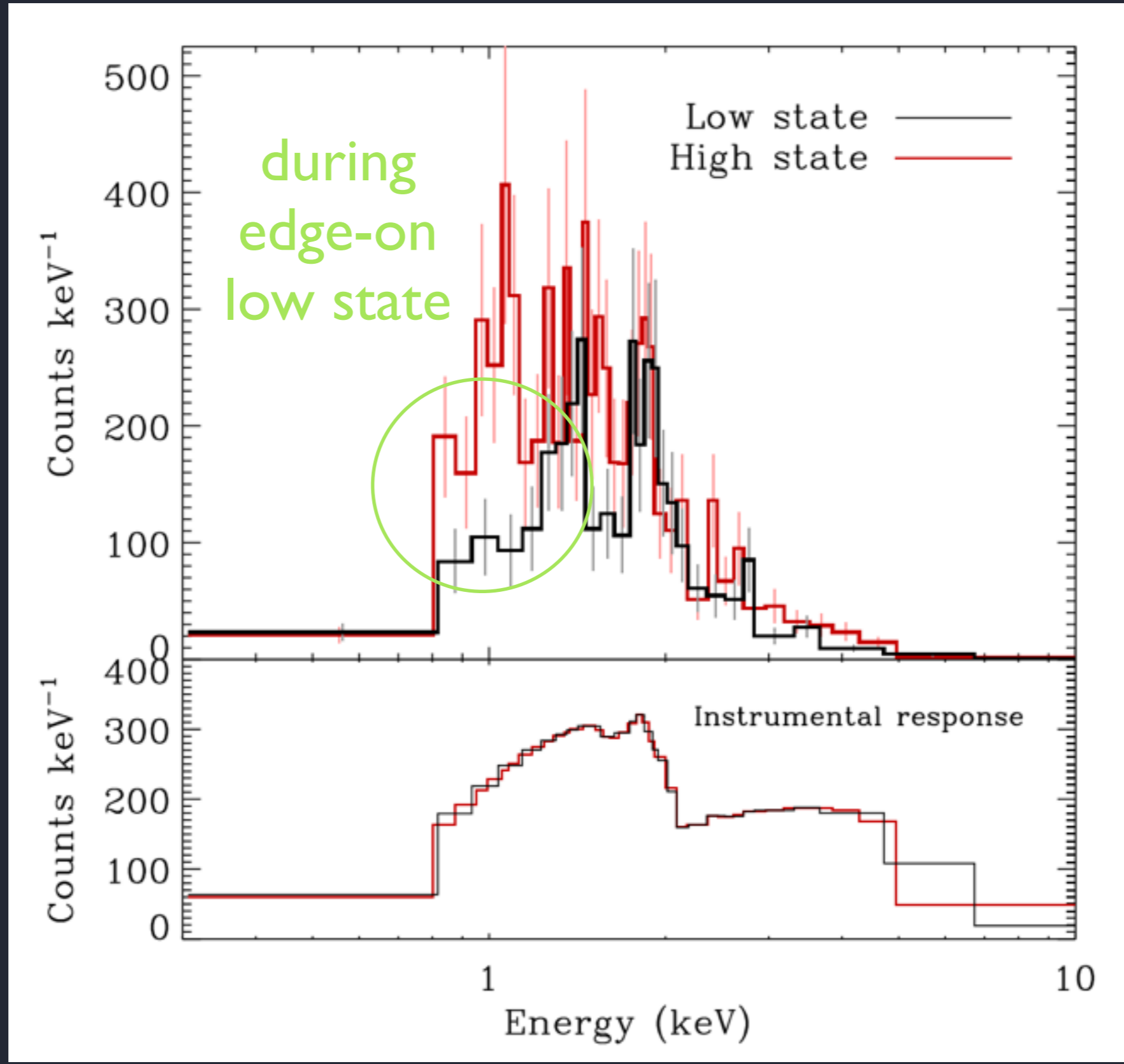


Figure 7. Spatial variation of optical depth for bound-free absorption of X-ray emission by both the cool downflow and wind outflow components of the ADM model, as well as by occultation of the opaque star. The top row shows results for a distant observer to the right, with an equator-on view, while the bottom row is for an observer at the top, with a pole-on view. The model assumes an apex smoothing length $h = 0.1R_*$, and a terminal speed $V_\infty = 3v_e$ for a corresponding unmagnetized wind. The left, middle and right columns show cases with a corresponding wind optical depth $\tau_* = 0.1, 0.3$ and 1 .

Spectral signature of absorption in NGC 1624-2

Of?p with giant magnetosphere

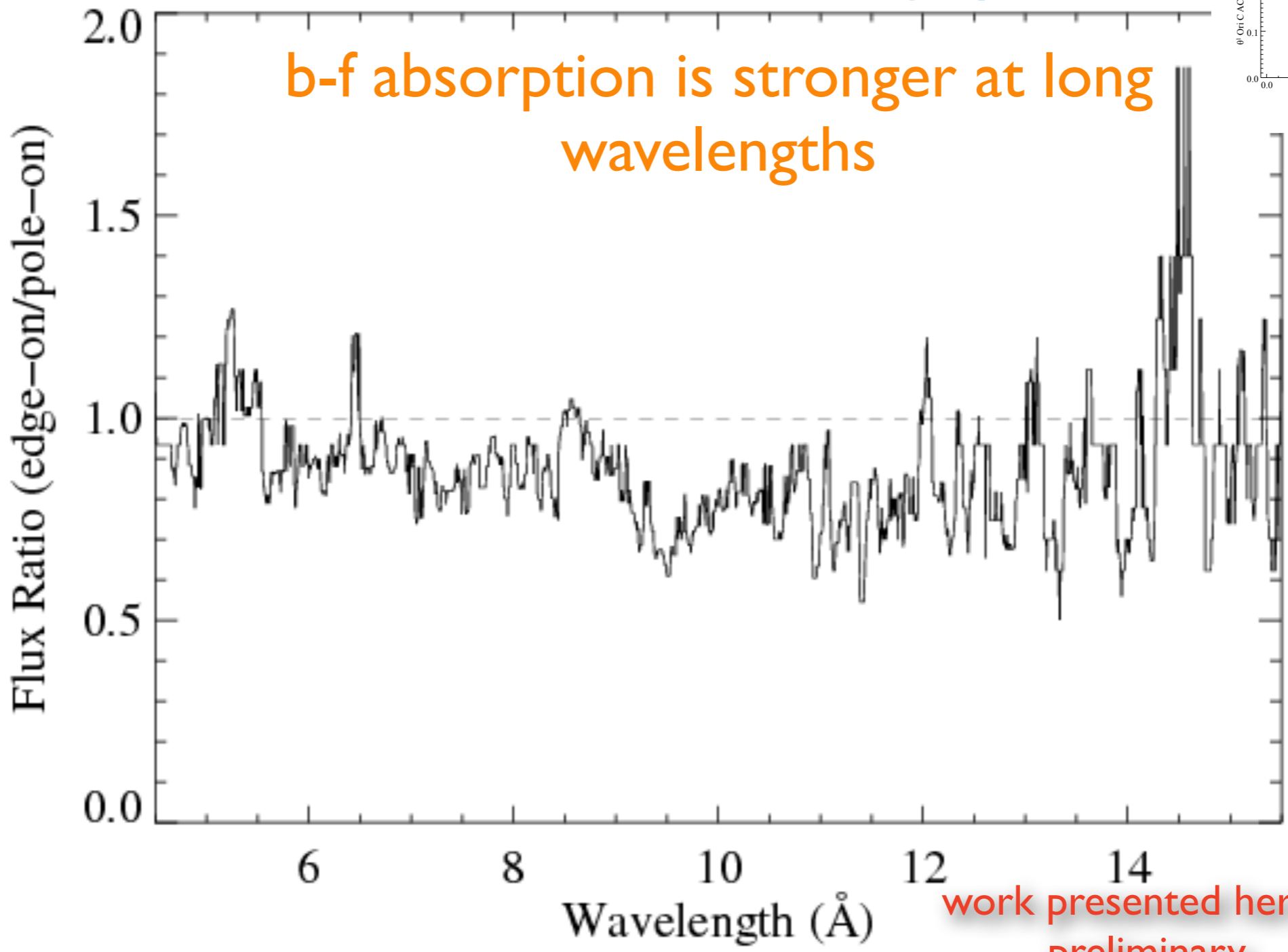


from V. Petit

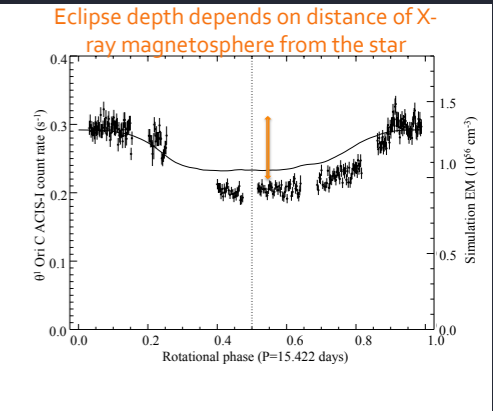
Ratio of edge-on to pole-on spectra for θ^1 Ori C

occultation should be gray

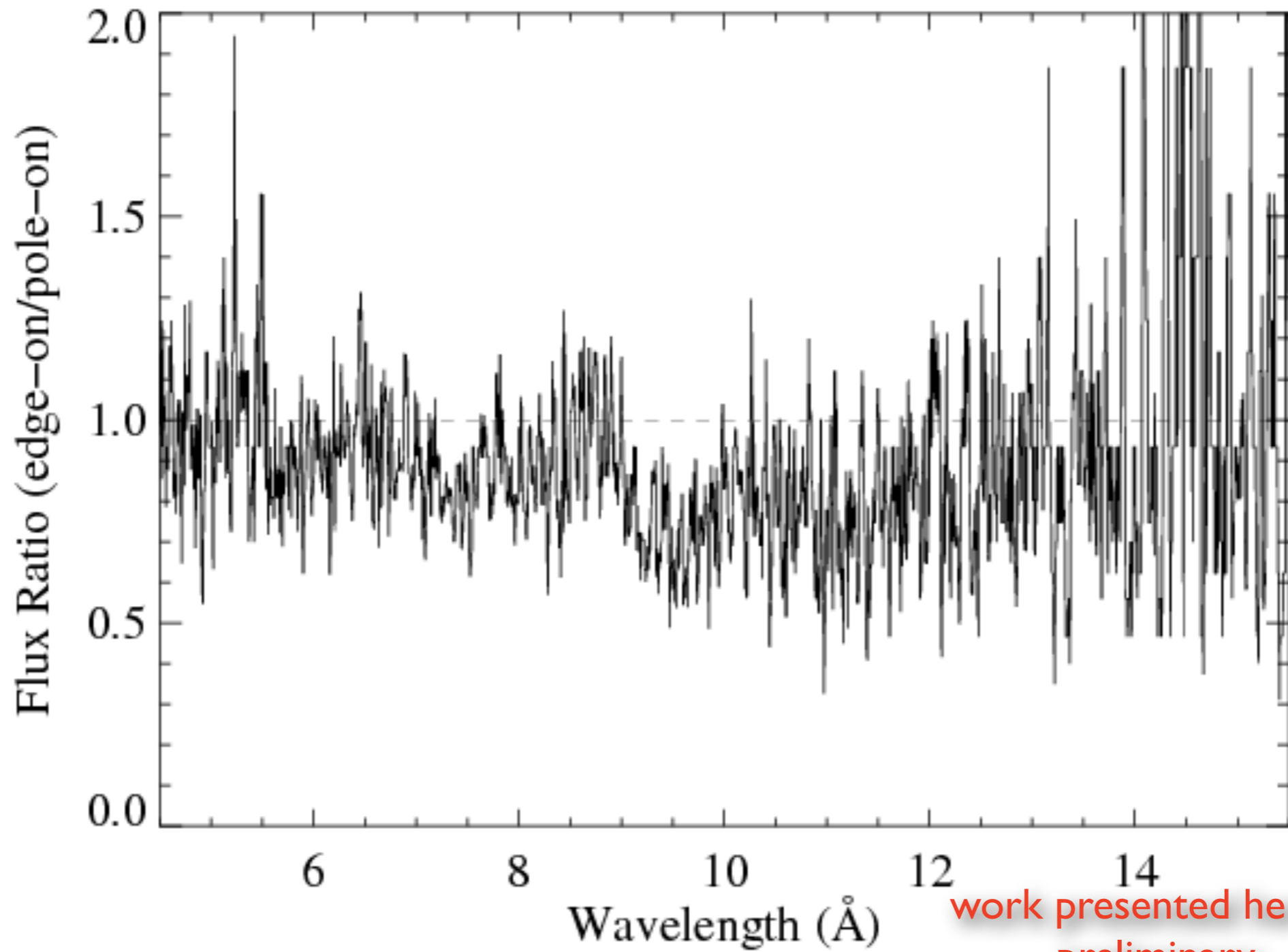
b-f absorption is stronger at long wavelengths



work presented here is preliminary

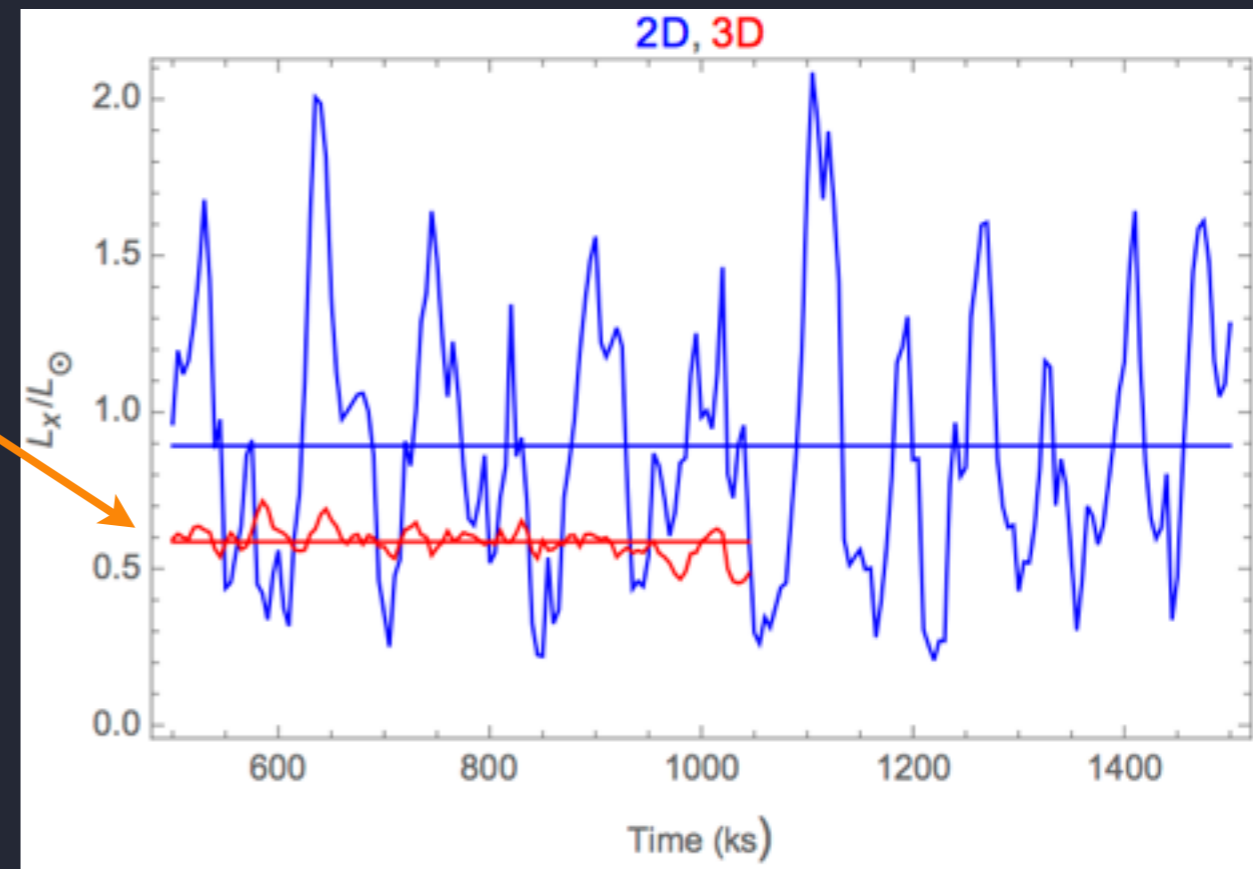
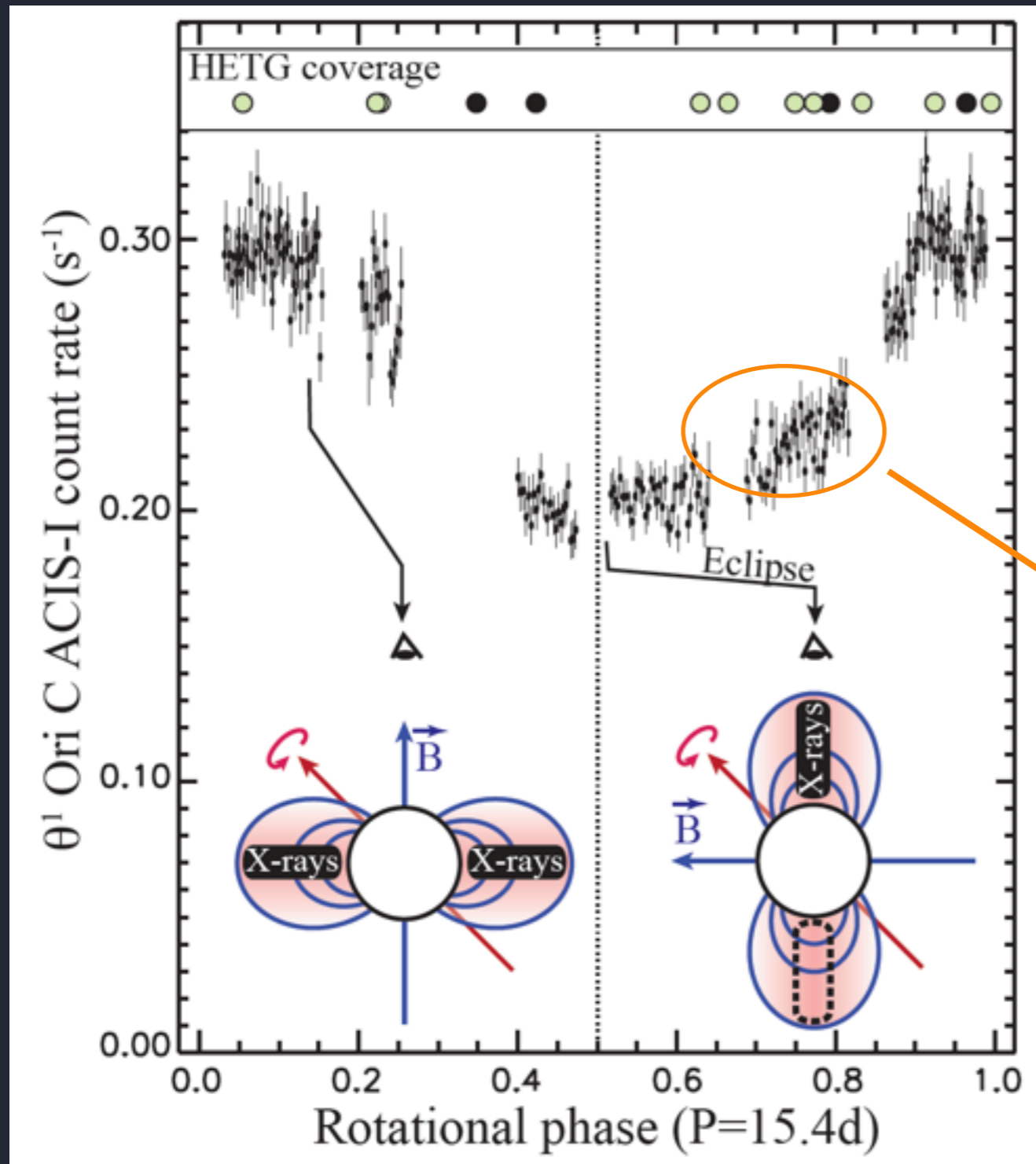


Ratio of edge-on to pole-on spectra for θ^1 Ori C



X-ray light curve: focus on the stochastic, short-term variability

variability of $< 10\%$
consistent with 3-D model:
lateral structure



Other magnetic O stars?

Other magnetic O stars: HD 191612 (Of?p)

X-ray luminosity almost as high as θ^1 Ori C

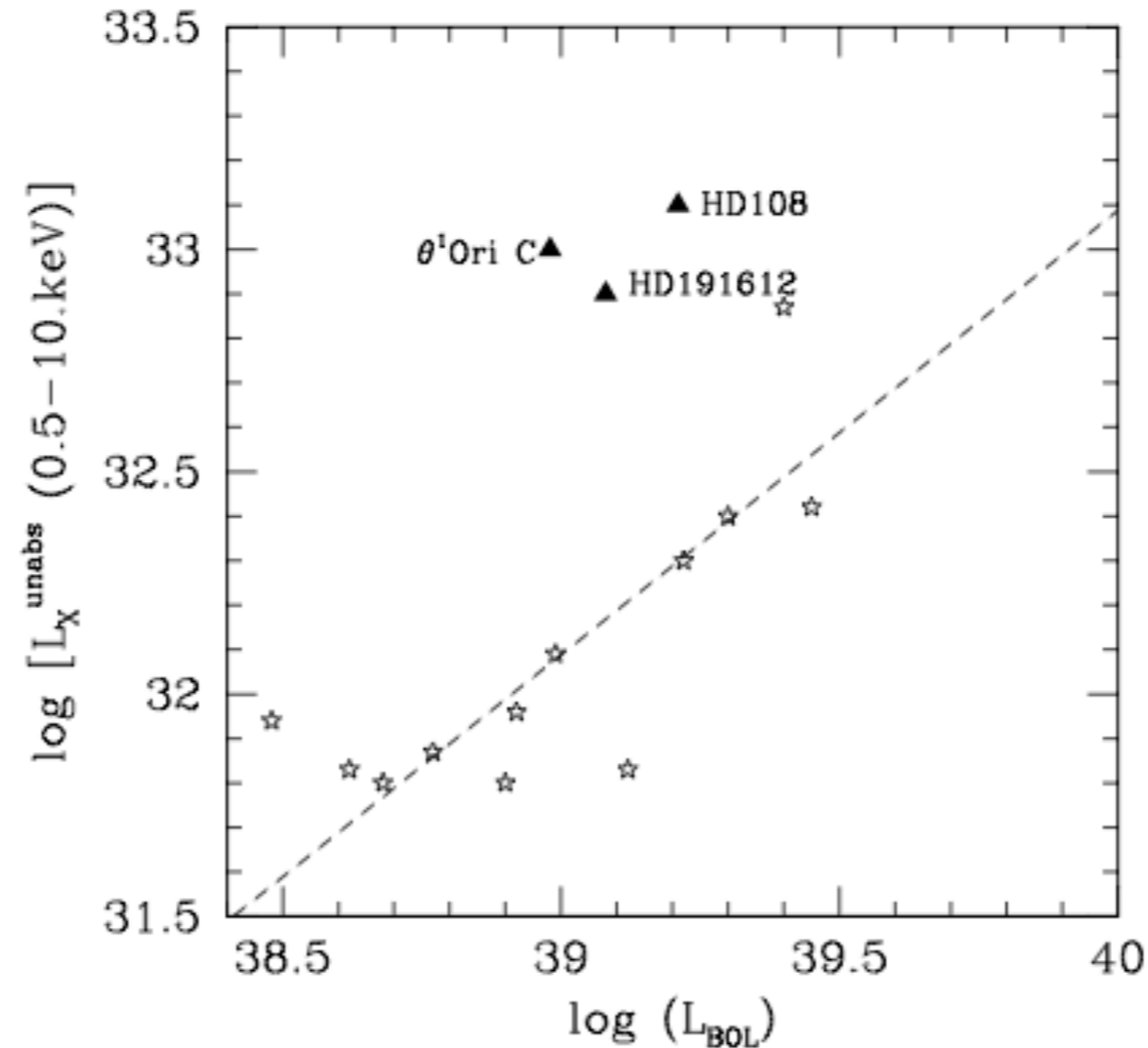
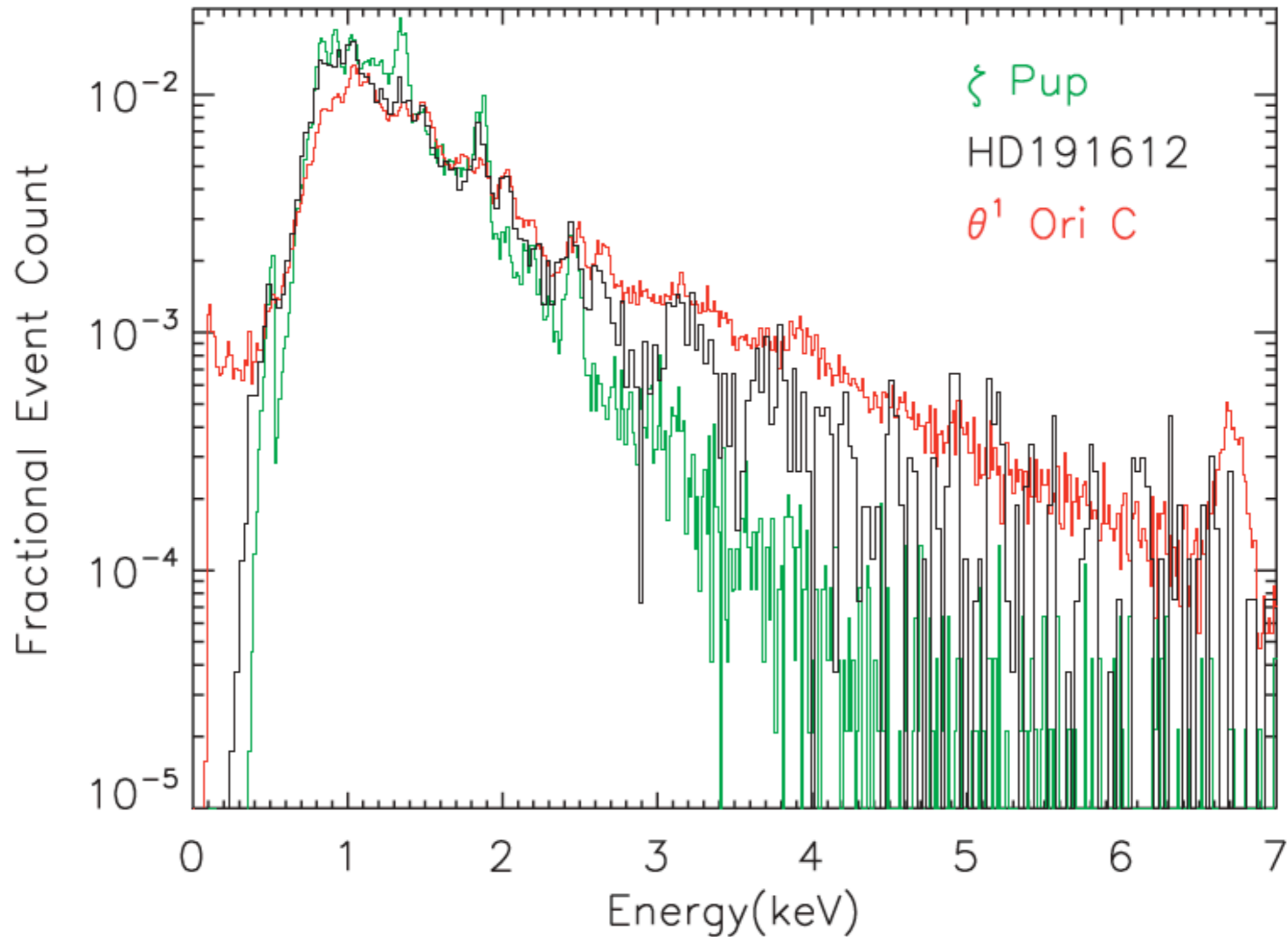


Figure 4. Diagram showing the X-ray luminosity (in erg s^{-1}) versus bolometric luminosity (in erg s^{-1}). The dashed line indicates the typical relation for O stars (from Sana et al. 2006); HD 108, HD 191612 and θ^1 Ori C all lie above it. Asterisks show the position of hot stars in NGC 6231 (Sana et al. 2006) with three outliers: the two objects lying above the line are CW binaries whereas the one lying below is a Wolf-Rayet binary.

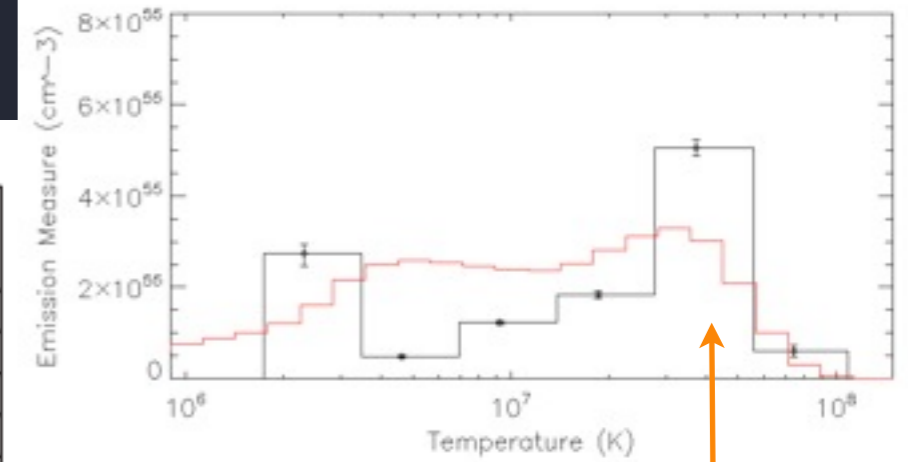
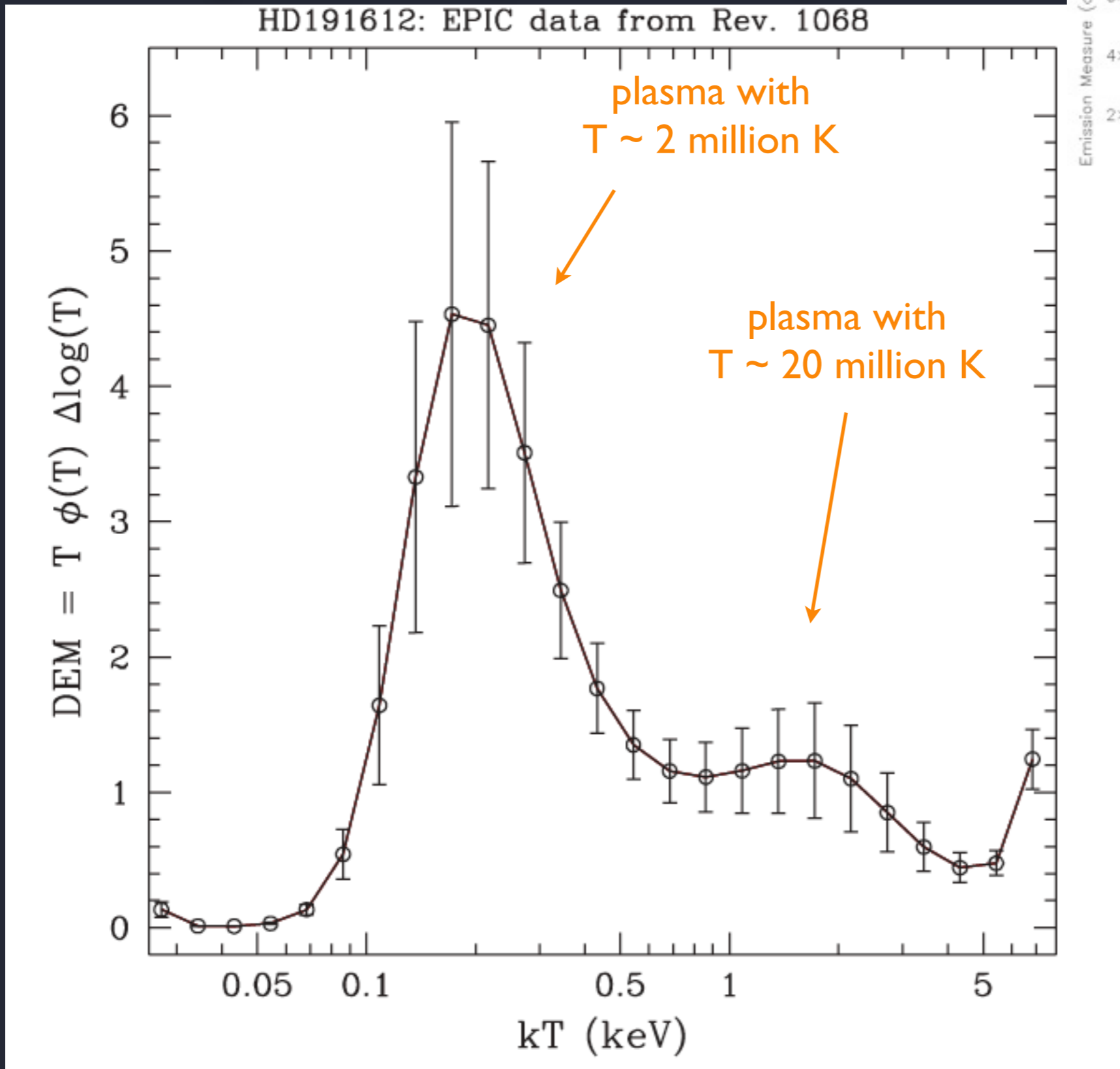
Broadband X-ray spectra: HD 191612

spectrum softer than θ^1 Ori C



HD 191612: some very hot plasma but mostly cooler (few 10^6 K)

θ^1 Ori C



$kT \sim 3$ keV
(35 million K)

Conclusions:

The MCWS scenario, and MHD simulations specifically, predict the observed amount of hot magnetospheric plasma and its temperature distribution

Mass-loss rate, wind speed, magnetic confinement are as expected

Future analysis: absorption, line widths - phase-dependence; also shock-heating rate from emission line strengths can constrain duty-cycle/efficiency ADM vs. MHD

What's different about other magnetic O stars with softer spectra and broader lines?